

## Supporting Information

### Domain-targeted metabolomics delineates the heterocycle assembly steps of colibactin biosynthesis

Eric P. Trautman<sup>1,2</sup>, Alan R. Healy<sup>1,2</sup>, Emilee E. Shine<sup>2,3</sup>, Seth B. Herzon<sup>1,4</sup>, Jason M. Crawford<sup>1,2,3,\*</sup>

<sup>1</sup>Department of Chemistry, Yale University, New Haven, Connecticut 06520, United States

<sup>2</sup>Chemical Biology Institute, Yale University, West Haven, Connecticut 06516, United States

<sup>3</sup>Department of Microbial Pathogenesis, Yale School of Medicine, New Haven, Connecticut 06536, United States

<sup>4</sup>Department of Pharmacology, Yale School of Medicine, New Haven, Connecticut 06520, United States

#### Table of Contents

1. Experimental Methods.....	S1-S6
2. Supplemental Tables.....	S7-S36
3. Supplemental Figures.....	S37-S45
4. Supplemental References.....	S46

## Experimental Methods

### Mutational inactivation of individual NRPS-PKS domains

Protein sequence alignments were generated to identify the active site residues of each NRPS-PKS domain, and these are shown in Figure S1. The mutations in each type of domain were made as follows. The conserved active site cysteine residues of ketosynthase (KS) domains were mutated to alanine. In the case of ClbI, the KS active site has a serine in place of a cysteine. This active site residue was mutated to the canonical cysteine residue and the inactivating alanine mutation. Acyl transferases (ATs) contain a consensus GxSxG active site motif. Serine to alanine mutations were generated to inactivate the AT domains. Carrier proteins in both NRPS and PKS contain a conserved serine residue, which is phosphopantetheinylated to generate their active holo-forms. These serine residues were mutated to alanine to prohibit posttranslational modification, and thus, abolish carrier protein activities. Condensation domains contain a conserved HHxxxDG active site motif, in which the second histidine acts as a general base.<sup>1</sup> These histidine residues were mutated to alanine to abolish activity.

The superfamily of adenylate-forming enzymes has a conserved TSGTTGKPKG motif.<sup>1</sup> This motif forms a flexible loop that interacts with the pyrophosphate leaving group. Mutation of the first glycine in this loop to a negatively charged aspartate has previously been shown to prevent adenylation activity.<sup>1</sup> This glycine was mutated in the A domains to aspartate.

Until recently, it was thought that a conserved DxxxxD motif in cyclization (Cy) domains was responsible for catalysis and that mutation of either aspartate to alanine would abolish activity. In our experiments, mutation of one aspartate reduced activity but did not abolish it, while mutation of both residues was sufficient to eliminate activity. A recent paper in which a cyclization domain was crystallized, showed that this motif is actually not in the active site.<sup>2</sup> Despite this, double mutation in the DxxxxD motif abolished Cy activity and was used in this study.

To the best of our knowledge, there has been no defining biochemical site-directed mutational inactivation studies of oxidase (Ox) domains in NRPS systems. However, the Ox domain falls into a superfamily of Nitro-FMN reductases, which require FMN as a cofactor. To abolish the activity of the Ox domain, a strategy where the FMN binding site was disrupted was employed. SWISS-MODEL was used to identify templates that shared structural similarity with the Ox domain. The FMN ligand was not modeled into the resulting structure, so the crystal structure of the closest homolog was used to identify residues important for FMN binding (Figure S2). Arginine and serine residues that are conserved across the family of FMN-dependent oxidoreductases were identified to form strong interactions with the phosphate of FMN. These two residues were individually mutated to glutamate to form an electrostatic repulsion with the phosphate and disrupt FMN binding. We analyzed both mutants. The arginine to glutamate mutation was more effective at abolishing activity than the serine to glutamate mutation.

### MAGE

Multiplex automated genome engineering (MAGE) was used to introduce point mutations on the bacterial artificial chromosome pBAC PKS<sup>3</sup> to individually inactivate select domains from the colibactin biosynthetic gene cluster. To do so, between three and five rounds of MAGE were performed on a high efficiency variant of EcNR1 containing pBAC PKS+. One round of MAGE was done as follows. First, 3 mL of Lysogeny Broth (LB) with 12.5 µg/mL chloramphenicol (CAM) was inoculated with overnight seed culture at a 1:200 ratio. The culture was grown at 37 °C until the OD<sub>600</sub> reached 0.4. Cultures were induced by incubating at 42 °C for 15 min. The cultures were split into 1 mL portions and cooled on ice. Cells were pelleted by spinning for 30 seconds at 21,000 × g at 4 °C. The supernatant was removed and cells were resuspended in 1 mL of chilled ddH<sub>2</sub>O. This process was repeated for a total of two washes before resuspending cells in 50 µL of chilled ddH<sub>2</sub>O. 1 µL of 50 µM oligonucleotide was added and cells were transferred to an electroporation cuvette with a 0.1 cm gap width. Cells were electroporated at 1800 V with 25 µF capacitance and 200Ω resistance. Transformed cells were recovered in 3 mL of LB + CAM at 30 or 34 °C until the OD<sub>600</sub> reached 0.4. At this point, cells were either induced for another MAGE cycle, let grow overnight to begin another cycle the next day, or plated on LB plates for screening.

### Primer design

MAGE oligonucleotides were designed as previously outlined<sup>4</sup> to introduce a single codon mutation. Oligonucleotides were designed to be 90 nucleotides long and contain two 5'-phosphorothioate modifications. The mutation was placed at least 10 nucleotides in from either end of the oligo. The oligo was designed to have a folding energy of greater than -12 kcal/mol as calculated by Mfold to minimize secondary structure.<sup>5</sup> For oligos with lower folding energies, more rounds of MAGE were performed to increase the proportion of mutant clones in the pool.

### Screening for mutants

Multiplex allele-specific colony PCR (MASC-PCR) was used to screen for mutations introduced by MAGE. Two primers were designed for each desired mutation, with the 3'-end of the primer matching either the wild-type or mutant sequence. The primer length was varied to keep the  $T_M$  of the two primers between 57-60 °C and within 1.5 °C of each other. Individual colonies were screened by PCR for introduction of the desired mutation, as described previously.<sup>4</sup> Mutants were validated by amplifying the gene of interest with overspanning PCR and sequencing.

### Construction of Deletion mutant $\Delta clbPO$

The  $\Delta clbO$  mutant was generated using the lambda Red recombinase system.<sup>6</sup> The FRT-flanked apramycin resistance cassette of plasmid pIJ773 was PCR amplified using primers with short sequence extensions homologous to the 5' and 3' ends of *clbO*. The PCR product was *DpnI*-digested, purified, and suspended in H<sub>2</sub>O. *E. coli* DH10B carrying recombineering plasmid pKD46 and pBAC-PKS were grown in LB with 100 µg/mL and 10 µM L-arabinose to an OD<sub>600</sub> of 0.6. The cells were pelleted by centrifugation and washed three times in ice-cold ddH<sub>2</sub>O. The cells were resuspended in 100 µL ice-cold ddH<sub>2</sub>O. Between 10 and 100 ng of PCR amplified apramycin resistance cassette was added to 25 µL of cells and transformed by electroporation (1800 V with 25 µF capacitance and 200Ω resistance). After 1.5 hours of phenotypic expression in 1 mL of LB at 30 °C, bacteria were plated on LB agar supplemented with 50 µg/mL apramycin and 12.5 µg/mL chloramphenicol and incubated at 30 °C for about 24 hours. Colonies were analyzed with overspanning PCR to confirm replacement of the gene of interest with the FRT-flanked antibiotic resistance cassette. Recombineering plasmid pKD46 was cured by growing respective colonies at 43 °C overnight, and the cassette was subsequently flipped out by transforming with plasmid pCP20 encoding the FLP recombinase. Successful deletion of the cassette in apramycin- and chloramphenicol-resistant colonies was confirmed by overspanning PCR. A point mutant in the peptidase *clbP* was subsequently generated on this strain through MAGE as previously described to obtain double mutant  $\Delta clbPO$ .

### Metabolomics

*E. coli* DH10B carrying pBAC, pBAC-PKS, or pBAC-PKS\* containing the point mutant(s) were grown overnight in LB+CAM. This overnight culture was used to inoculate 5 replicates of 5 mL of production media at a 1:200 dilution (Difco M9 + 2 mM MgSO<sub>4</sub> + 0.1 mM CaCl<sub>2</sub> + 5 g/L casamino acids + 0.4% glucose + 12.5 µg/mL CAM + 1 g/L of each of the following amino acids: L-serine, L-cysteine, L-alanine, L-valine, and L-asparagine). Cultures were grown at 37 °C with 250 rpm shaking to an OD<sub>600</sub> of 0.4-0.6. Cultures were cooled on ice for approximately 10 minutes before inducing with isopropyl- $\beta$ -D-galactopyranoside (IPTG) at a final concentration of 0.2 mM. Cultures were incubated at 25 °C for 42 hours before extraction. To extract, 5 mL of ethyl acetate (EtOAc) was added to the culture. Cultures were vortexed for 15-30 seconds each. The layers then were separated by centrifugation (3000 rpm × 10 min). The top 4 mL of the EtOAc layer was removed and transferred to a glass vial. The EtOAc was removed *in vacuo*. Dried extracts were dissolved in 0.5 mL of MeOH for metabolomic analysis. Due to the instability of several metabolites, extracts were immediately analyzed, and experiments were

performed in 4 sets: ClbH and ClbI mutants with a wild-type ClbP background; ClbH, ClbI, ClbL, and ClbQ mutants in a ClbP point mutant background; ClbJ mutants in a ClbP point mutant background; ClbK mutants in a ClbP point mutant background; and  $\Delta ClbPO$  mutants. Each set of experiments was normalized to the average abundance of ClbP or wild-type controls.

### Data acquisition

High-resolution mass spectrometry (HRMS) data was collected using an Agilent iFunnel 6550 Quadrupole-Time-of-Flight Mass Spectrometer (QTOF-MS) with an electrospray ionization (ESI) source. The mass spectrometer was coupled to an Agilent Infinity 1290 ultra-performance liquid chromatogram (UPLC). Separation of metabolites prior to MS acquisition was done using a Phenomenex Kinetex 1.7  $\mu$ M C18 100 Å column (100  $\times$  2.1 mm) with a water/acetonitrile (MeCN) gradient with 0.1% formic acid as an additive. The gradient used was as follows: 0-2 min 5% MeCN; 2-26 min 5-98% MeCN; hold at 98% for 7 min. The column temperature was kept at 25 °C with a flowrate of 0.3 mL/min. Mass spectra were gathered using Dual Agilent Jet Stream (AJS) ESI in positive mode. The mass range was set from 100 m/z to 1500 m/z with a scan speed of 1 scan/second. The capillary and nozzle voltages were set to 4000 V and 2000 V, respectively. The source parameters were set with a gas temperature of 225 °C and a flow rate of 15 L/min, nebulizer at 20 psig, and sheath gas temperature at 275 °C at a flow of 12 L/min. MS data were acquired with MassHunter Workstation Data Acquisition (Version B.06.01, Agilent Technologies). Data was analyzed using MassHunter Qualitative Analysis (Version B.06.00, Agilent Technologies). To quantify production levels of ions of interest, the exact mass was extracted with a 10 ppm window of error. EICs were integrated for each of the five replicates and normalized to the average abundance of the metabolite in the ClbP samples.

### Cyclization of linear Precolibactin C

Linear precolibactin **7** was obtained via synthesis as previously reported.<sup>7</sup> To perform the cyclization reaction, 0.3 mg of **7** was dissolved in 50  $\mu$ L DMSO containing potassium carbonate (3 mg/mL solution, 3.0 equivalents). The reaction was incubated at room temperature for 4 hours then diluted 1:1000 with MeOH for LC-MS analysis.

### Isotopic labeling of precolibactin thiazoline **4**

*E. coli* DH10B carrying pBAC, pBAC-PKS, or pBAC-PKS\* with individual point mutants were grown overnight in LB+CAM. This overnight culture was used to inoculate 3 replicates of 5 mL of production media at a 1:200 dilution (Difco M9 + 2 mM MgSO<sub>4</sub> + 0.1 mM CaCl<sub>2</sub> + 5 g/L casamino acids + 0.4% glucose + 12.5  $\mu$ g/mL CAM + 4% (w/v) L-[U-<sup>13</sup>C]-cysteine + 1 g/L of each of the following amino acids: L-serine, L-alanine, L-valine, and L-asparagine). Cultures were grown at 37 °C with 250 rpm shaking to an OD<sub>600</sub> of 0.4-0.6. Cultures were cooled on ice for approximately 10 minutes before inducing with isopropyl- $\beta$ -D-galactopyranoside (IPTG) at a final concentration of 0.2 mM. Cultures were incubated at 25 °C for 42 hours before extraction. Extraction and metabolomic analysis was performed as described above.

### Cleavage of **2** to confirm the structures of S23 and S24

25  $\mu$ L of an overnight 5 mL culture of pBAD18 or pPEB018 (pClbP) in LB + 100  $\mu$ g/mL Amp was used to inoculate 5 mL of fresh LB + 100  $\mu$ g/mL Amp. Cultures were incubated at 37 °C with 250 rpm shaking until the OD<sub>600</sub> of the culture was between 0.4 and 0.5. At this point, L-arabinose (final concentration 0.01%) was added to induce protein expression. Cultures were incubated at 37 °C for 30 min. The synthetic substrate, **2**, was dissolved in DMSO to a concentration of 10 mM. 5  $\mu$ L of substrate solution was added (final concentration of 10  $\mu$ M) and incubated at 37 °C. After four hours, 2.5 mL aliquots were removed and extracted with 5 mL EtOAc. Samples were vortexed for 20 seconds, centrifuged (3000 rpm, 10 min) to separate the layers, and 4 mL EtOAc were removed and dried *in vacuo*. The remaining 2.5 mL of unextracted culture was incubated for an additional four hours before extracting

as above. The dried samples were dissolved in 0.5 mL MeOH for LC-MS analysis. Cleavage of **2** is shown in Figure S3.

#### **Cleavage of 7 by ClbP**

Starter cultures of pBAD18 or pPEB018 were inoculated into 5 mL of LB + 100 µg/mL Amp. 25 µL of an overnight 5 mL culture of pBAD18 or pPEB018 (pClbP) in LB + 100 µg/mL Amp was used to inoculate 5 mL of fresh LB + 100 µg/mL Amp. Cultures were incubated at 37 °C with 250 rpm shaking until the OD<sub>600</sub> of the culture was between 0.4 and 0.5. L-arabinose (final concentration 0.01%) was added to induce protein expression. Cultures were incubated at 37 °C for 30 min. The synthetic substrate **7** was dissolved in DMSO to a concentration of 5 mM. 50 µL of substrate solution was added (final concentration 50 µM) and incubated at 37 °C for 24 hours. After 24 hours, the cultures were extracted with 5 mL butanol (BuOH). Samples were vortexed for 20 seconds, centrifuged (3000 rpm, 10 min) to separate the layers, and 4 mL BuOH were removed and dried *in vacuo*. The dried samples were dissolved in 0.5 mL MeOH for LC-MS analysis. LC-MS analysis was performed as detailed above with a water/MeCN gradient with 0.1% formic acid additive; however, the gradient used was as follows: 0 – 2 min: 5 % MeCN; 2 – 15 min ramp from 5 – 28% MeCN; 15 – 26 min, ramp from 28 – 98% MeCN.

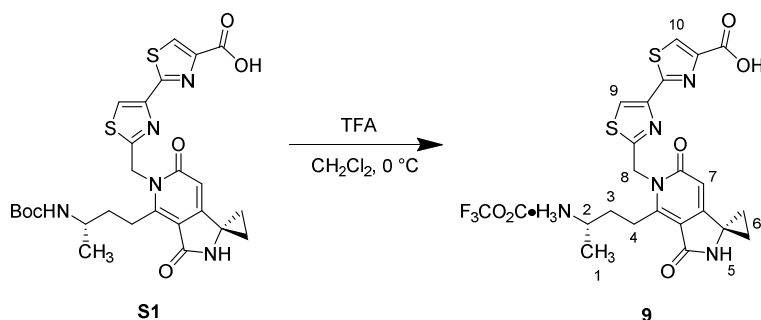
**General Experimental Procedures.** All reactions were performed in single-neck, flame-dried, round-bottomed flasks fitted with rubber septa under a positive pressure of nitrogen unless otherwise noted. Air- and moisture-sensitive liquids were transferred via syringe or stainless steel cannula. Organic solutions were concentrated by rotary evaporation at 28–32 °C.

**Materials.** Commercial solvents and reagents were used as received with the following exceptions. Dichloromethane was purified according to the method of Pangborn et al.<sup>8</sup> 2'-((3-(1-((*S*)-6-((*R*)-4-amino-4-oxo-2-tetradecanamidobutanamido)-3-oxoheptanamido)cyclopropyl)-3-oxopropanamido)methyl)-[2,4'-bithiazole]-4-carboxylic acid (**7**),<sup>7</sup> (*S*)-2'-((4'-(3-((*tert*-butoxycarbonyl)amino)butyl)-3',6'-dioxo-2',3'-dihydrospiro[cyclopropane-1,1'-pyrrolo[3,4-*c*]pyridin]-5'(6'*H*)-yl)methyl)-[2,4'-bithiazole]-4-carboxylic acid (**S1**),<sup>9</sup> and (*S,Z*)-2'-((3-(1-(2-(1-(*tert*-butoxycarbonyl)-5-methylpyrrolidin-2-ylidene)acetamido)cyclopropyl)-3-oxopropanamido)methyl)-[2,4'-bithiazole]-4-carboxylic acid (**S2**)<sup>9</sup> were prepared according to published procedures.

**Instrumentation.** Proton nuclear magnetic resonance spectra (<sup>1</sup>H NMR) were recorded at 600 MHz at 24 °C, unless otherwise noted. Chemical shifts are expressed in parts per million (ppm, δ scale) downfield from tetramethylsilane and are referenced to residual protium in the NMR solvent (C<sub>2</sub>D<sub>6</sub>OS, δ 2.50). Data are represented as follows: chemical shift, multiplicity (s = singlet, d = doublet, t = triplet, q = quartet, m = multiplet and/or multiple resonances, br = broad, app = apparent), coupling constant in Hertz, integration, and assignment. Proton-decoupled carbon nuclear magnetic resonance spectra (<sup>13</sup>C NMR) were recorded at 151 MHz at 24 °C, unless otherwise noted. Chemical shifts are expressed in parts per million (ppm, δ scale) downfield from tetramethylsilane and are referenced to the carbon resonances of the solvent (C<sub>2</sub>D<sub>6</sub>OS, δ 39.5). Signals of protons and carbons were assigned, as far as possible, by using the following two-dimensional NMR spectroscopy techniques: [<sup>1</sup>H, <sup>1</sup>H] COSY (Correlation Spectroscopy), [<sup>1</sup>H, <sup>13</sup>C] HSQC (Heteronuclear Single Quantum Coherence) and long range [<sup>1</sup>H, <sup>13</sup>C] HMBC (Heteronuclear Multiple Bond Connectivity).

## Synthetic Procedures.

### Synthesis of the pyridone **9**:

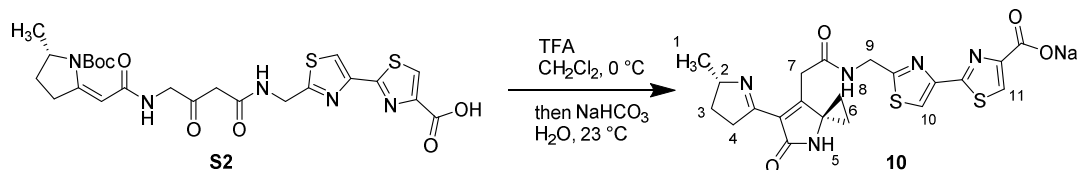


Trifluoroacetic acid (100 μL, 1.36 mmol, 130 equiv) was added dropwise via syringe to a solution of the amide **S1** (6.0 mg, 10.5 μmol, 1 equiv) in dichloromethane (300 μL) at 0 °C. The reaction mixture was stirred for 3 h at 0 °C. The reaction mixture was concentrated to provide the pyridone **9** as a white solid. The product so obtained was used without further purification.

<sup>1</sup>H NMR (600 MHz, DMSO-*d*<sub>6</sub>) δ 8.63 (s, 1H, H<sub>5</sub>), 8.48 (s, 1H, H<sub>10</sub>), 8.30 (s, 1H, H<sub>9</sub>), 7.82 (bs, 3H), 6.24 (s, 1H, H<sub>7</sub>), 5.60 (d, *J* = 16.2 Hz, 1H, H<sub>8</sub>), 5.56 (d, *J* = 16.2 Hz, 1H, H<sub>8</sub>), 3.53 – 3.47 (m, 1H, H<sub>4</sub>), 3.47 – 3.39 (m, 1H, H<sub>4</sub>), 3.35 – 3.21 (m, 1H, H<sub>2</sub>), 1.99 – 1.86 (m, 1H, H<sub>3</sub>), 1.86 – 1.77 (m, 1H, H<sub>3</sub>), 1.40 (app t, *J* = 2.8 Hz, 2H, H<sub>6</sub>), 1.38 (app t, *J* = 2.8 Hz, 2H, H<sub>6</sub>), 1.24 (d, *J* = 6.6 Hz, 3H, H<sub>1</sub>). <sup>13</sup>C NMR (151 MHz, DMSO-*d*<sub>6</sub>) δ 166.9 (C), 166.8 (C), 162.0 (C), 161.9 (C), 161.8 (C), 159.6 (C), 151.6 (C), 148.2 (C), 146.9 (C), 129.1 (CH), 119.3 (CH), 109.9 (C), 103.9 (CH), 46.5 (CH), 44.4 (CH<sub>2</sub>), 39.9 (C), 33.5 (CH<sub>2</sub>), 23.2

(CH<sub>2</sub>), 18.1 (CH<sub>3</sub>), 15.3 (CH<sub>2</sub>), 15.2 (CH<sub>2</sub>). HRMS-Cl (m/z): [M + H]<sup>+</sup> calcd for C<sub>21</sub>H<sub>22</sub>N<sub>5</sub>O<sub>4</sub>S<sub>2</sub>, 472.1108; found, 472.1114.

*Synthesis of the lactam 10:*



Trifluoroacetic acid (100  $\mu$ L, 1.35 mmol, 133 equiv) was added dropwise via syringe to a solution of the amide **S2** (6.0 mg, 10.2  $\mu$ mol, 1 equiv) in dichloromethane (300  $\mu$ L) at 0 °C. The reaction mixture was stirred for 3 h at 0 °C. The reaction mixture was concentrated. The concentrated reaction mixture was diluted with saturated aqueous sodium bicarbonate solution (200  $\mu$ L). The diluted reaction mixture was stirred for 1 h at 23 °C. The reaction mixture was concentrated. The residue was concentrated from benzene (2  $\times$  300  $\mu$ L) to provide the lactam **10** as a white solid. The product so obtained was used without further purification.

<sup>1</sup>H NMR (600 MHz, DMSO-*d*<sub>6</sub>)  $\delta$  10.30 (t, *J* = 6.0 Hz, 1H, H<sub>8</sub>), 8.65 (bs, 1H, H<sub>5</sub>), 8.43 (s, 1H, H<sub>10</sub>), 7.84 (s, 1H, H<sub>11</sub>), 4.60 (dd, *J* = 6.0, 3.3 Hz, 2H, H<sub>9</sub>), 4.16 – 4.08 (m, 1H, H<sub>2</sub>), 3.32 (d, *J* = 6.7 Hz, 2H, H<sub>7</sub>), 3.10 (dddd, *J* = 18.0, 9.8, 4.7, 2.2 Hz, 1H, H<sub>4</sub>), 2.87 (dddd, *J* = 18.0, 9.9, 7.8, 2.0 Hz, 1H, H<sub>4</sub>), 2.16 – 2.02 (m, 1H, H<sub>3</sub>), 1.76 – 1.63 (m, 2H, H<sub>6</sub>), 1.42 – 1.31 (m, 3H, H<sub>3</sub>, H<sub>6</sub>), 1.19 (d, *J* = 6.7 Hz, 3H, H<sub>1</sub>). <sup>13</sup>C NMR (151 MHz, DMSO-*d*<sub>6</sub>)  $\delta$  170.3 (C), 169.7 (C), 168.4 (C), 168.2 (C), 160.3 (C), 158.8 (C), 157.7 (C), 148.2 (C), 127.4 (C), 121.8 (CH), 117.0 (CH), 66.6 (CH), 45.3 (C), 40.4 (CH<sub>2</sub>), 36.6 (CH<sub>2</sub>), 33.6 (CH<sub>2</sub>), 29.7 (CH<sub>2</sub>), 21.9 (CH<sub>3</sub>), 11.9 (CH<sub>2</sub>), 11.8 (CH<sub>2</sub>). HRMS-Cl (m/z): [M + H]<sup>+</sup> calcd for C<sub>21</sub>H<sub>22</sub>N<sub>5</sub>O<sub>4</sub>S<sub>2</sub>, 472.1108; found, 472.1109.

## Supplemental Tables

**Table S1. Strains and Plasmids**

Strains	Genotype	Reference
<i>E. coli</i> DH10B	F- mcrA _(mcrBC-hsdRMS-mrr) [_80d_lacZ_M15] _lacX74 deoR recA1 endA1 araD139_(ara,leu)7697 galU galK _ rpsL nupG	Invitrogen
High-efficiency variant of EcNR1	MG1655 Δ(ybhB-bioAB)::[λcI857 N(cro-pL,bet)::tetR-bla]) mutS::toIC	Strain provided by the Isaacs lab at Yale. EcNR1 parent <sup>4</sup>
<b>Plasmids</b>		
pBAC-empty	pBeloBAC11 without insert	( <sup>3</sup> )
pBAC-PKS	genomic fragment of <i>E. coli</i> IHE3034 encoding the complete colibactin <i>pks</i> island cloned into pBeloBAC11	( <sup>3</sup> )
pBAC-PKS ClbH G162D	pBAC-PKS with an inactivating mutation in ClbH-A1	This study
pBAC-PKS ClbH H662A	pBAC-PKS with a non-active site histidine mutated in ClbH-C	This study
pBAC-PKS ClbH H665A	pBAC-PKS with an inactivating mutation in ClbH-C	This study
pBAC-PKS ClbH G1137D	pBAC-PKS with an inactivating mutation in ClbH-A2	This study
pBAC-PKS ClbH S1524A	pBAC-PKS with an inactivating mutation in ClbH-T	This study
pBAC-PKS ClbI S178A	pBAC-PKS with an inactivating mutation in ClbI-KS	This study
pBAC-PKS ClbI S178C	pBAC-PKS with an active site mutation to cysteine in ClbI-KS	This study
pBAC-PKS ClbI S625A	pBAC-PKS with an inactivating mutation in ClbI-AT	This study
pBAC-PKS ClbI S952A	pBAC-PKS with an inactivating mutation in ClbI-T	This study
pBAC-PKS ClbP S95A	pBAC-PKS with an inactivating mutation in ClbP	This study
pBAC-PKS ClbP S95A ClbH G162D	pBAC-PKS with inactivating mutations in ClbP and ClbH-A1	This study
pBAC-PKS ClbP S95A ClbH H662A	pBAC-PKS with an inactivating mutation in ClbP and a non-active site histidine mutated in ClbH-C	This study
pBAC-PKS ClbP S95A ClbH H665A	pBAC-PKS with inactivating mutations in ClbP and ClbH-C	This study
pBAC-PKS ClbP S95A ClbH G1137D	pBAC-PKS with inactivating mutations in ClbP and ClbH-A2	This study
pBAC-PKS ClbP S95A ClbH S1524A	pBAC-PKS with inactivating mutations in ClbP and ClbH-T	This study
pBAC-PKS ClbP S95A ClbI S178A	pBAC-PKS with inactivating mutations in ClbP and ClbI-KS	This study
pBAC-PKS ClbP S95A ClbI S178C	pBAC-PKS with an inactivating mutation in ClbP and mutation of ClbI-KS active site to cysteine	This study
pBAC-PKS ClbP S95A ClbI S625A	pBAC-PKS with inactivating mutations in ClbP and ClbI-AT	This study
pBAC-PKS ClbP S95A ClbI S952A	pBAC-PKS with inactivating mutations in ClbP and ClbI-T	This study



pBAC-PKS ClbP S95A ClbJ H175A	pBAC-PKS with inactivating mutations in ClbP and ClbJ-C	This study
pBAC-PKS ClbP S95A ClbJ G650D	pBAC-PKS with inactivating mutations in ClbP and ClbJ-A1	This study
pBAC-PKS ClbP S95A ClbJ S1033A	pBAC-PKS with inactivating mutations in ClbP and ClbJ-T1	This study
pBAC-PKS ClbP S95A ClbJ D1226A	pBAC-PKS with inactivating mutations in ClbP and ClbJ-Cy	This study
pBAC-PKS ClbP S95A ClbJ D1231A	pBAC-PKS with inactivating mutations in ClbP and ClbJ-Cy	This study
pBAC-PKS ClbP S95A ClbJ D1226A D1231A	pBAC-PKS with inactivating mutations in ClbP and ClbJ-Cy	This study
pBAC-PKS ClbP S95A ClbJ G1697A	pBAC-PKS with inactivating mutations in ClbP and ClbJ-A2	This study
pBAC-PKS ClbP S95A ClbJ S2095A	pBAC-PKS with inactivating mutations in ClbP and ClbJ-T2	This study
pBAC-PKS ClbP S95A ClbK C167A	pBAC-PKS with inactivating mutations in ClbP and ClbK-KS	This study
pBAC-PKS ClbP S95A ClbK S747A	pBAC-PKS with inactivating mutations in ClbP and ClbK-T2	This study
pBAC-PKS ClbP S95A ClbK D939A	pBAC-PKS with inactivating mutations in ClbP and ClbK-Cy	This study
pBAC-PKS ClbP S95A ClbK D944A	pBAC-PKS with inactivating mutations in ClbP and ClbK-Cy	This study
pBAC-PKS ClbP S95A ClbK D939A D944A	pBAC-PKS with inactivating mutations in ClbP and ClbK-Cy	This study
pBAC-PKS ClbP S95A ClbK G1411A	pBAC-PKS with inactivating mutations in ClbP and ClbK-A2	This study
pBAC-PKS ClbP S95A ClbK R1768E	pBAC-PKS with inactivating mutations in ClbP and ClbK-Ox	This study
pBAC-PKS ClbP S95A ClbK S1770E	pBAC-PKS with inactivating mutations in ClbP and ClbK-Ox	This study
pBAC-PKS ClbP S95A ClbK S2073A	pBAC-PKS with inactivating mutations in ClbP and ClbK-T2	This study
pBAC-PKS ClbP S95A ClbL S179A	pBAC-PKS with inactivating mutations in ClbP and ClbL	This study
pBAC-PKS ClbP S95A ClbQ S78A	pBAC-PKS with inactivating mutations in ClbP and ClbQ	This study
pBAC-PKS ClbP S95A $\Delta clbO$	pBAC-PKS <i>clbO:FRT</i> with an inactivating mutation in ClbP	This study
pBAD18	Expression vector with araBAD promoter for induction with arabinose	( <sup>10</sup> )
pPEB018	<i>clbP</i> gene cloned into pBAD18	( <sup>11</sup> )

**Table S2. Primers used in this study**

<b>MAGE Primer</b>	<b>Sequence</b>	<b>Purpose</b>
clbP-ser-r	g*g*ctagtcagaaagcgaataactctagacacagtttacgagctgggaGC Gatgagtaaggcgtttaccggacttgggtgcaaatactgat	Inactivation of ClbP
ClbH-A1 G162D	a*t*tatttacacctccGATccaccgggtgccttaaagggtggcgacgg aacatgcagcgtgctaaaccgaattgtctggatgcagaac	Inactivation of ClbH-A <sub>1</sub>
ClbH-C H665A	g*t*agcgtattgttattcatctgcacGCCatcatcagtgatggctgctg aaaggcgtttgttacgcgaattgcaggccgcataaacg	Inactivation of ClbH-C
ClbH-A2 G1137D	a*a*cctgccagttagttgcccagatgcttttagattgcatgcccgtggtg atctttacctccGATactaccggcagccaaaggcgtc	Inactivation of ClbH-A <sub>2</sub>
ClbH-T S1524A	a*a*tttcttgatctcggtggacacGCActtctgctagtagatgcagca atacatcgggcagcagtgccgtcagcacgtggcgttggtt	Inactivation of ClbH-T
ClbI-KS S178A	a*t*cgctatcacctcaacctgcgcggccggcgatcacggctgcagactt ccGCGtcgacatccttgggtggcgtgctgctggcatgcaa	Inactivation of ClbI-KS
ClbI-AT S625A	t*t*gtggctcagttgggaatcacgcaacgtaagtattggtcatGCCc tgggcgaatgggtggcagcgacgttggcaggcgtgttctct	Inactivation of ClbI-AT
ClbI-T S952A	g*a*cggcttgggcattgacgacaacttctcgaagctggcggacatGCG ttgatgctgggcagttgctggcgcaggtacaggaacgggtc	Inactivation of ClbI-T
ClbJ-H175A	a*g*catactgctgctgtaactcatcgaacaatagccgtaacgagatacctg cgatgatgatGGCgtgcgcgcaaaacaccaaatagacaacc	Inactivation of ClbJ-C
ClbJ-G650D	a*a*cgcacacgccttttaggttaccgggtactATCGgaggtaaacaacag gtaggcctgcatatccggcaacagcgcgcaaggtgtagaata	Inactivation of ClbJ-A <sub>1</sub>
ClbJ-S1033A	g*a*tctctgctaccaacgttaccgccaacagTGCatgtcccccaagcg aaagaaatcgactcaggatcgacgtttttatcggcaata	Inactivation of ClbJ-T <sub>1</sub>
ClbJ-D1226A	t*a*cagcatcatcaactcctgctgtagcgtgcgcatactcagagcatcggc aatcagcagGGCgagactgaaatgcaagcggccatgttgc	Inactivation of ClbJ-Cy
ClbJ-D1231A	c*a*acatggccgcttgcattcagctcgtatctgattgccGCCgctct gagtatgcccagcgtacagcaggagttgatgatgctgtac	Inactivation of ClbJ-Cy
ClbJ-D2	g*c*acatggccgcttgcatttcaagtcGCCctgctgattgccGCCgc tctgagtatgcccagcgtacagcaggagttgatgatgctgta	Inactivation of ClbJ-Cy
ClbJ-G1679D	t*g*gtcgtatcactccttccgggtaccgggtggaATCGgaagtgaaa atgatataggccagatccgtgacatcccagccactcagcgc	Inactivation of ClbJ-A <sub>2</sub> and ClbK-A
ClbJ-S2095A	c*t*taaaaatctcctcaatacggcgatgcaacagcagcagatcggatGGC gcccggccgcttcaaaaaagttgctcattcagtcgatctg	Inactivation of ClbJ-T <sub>2</sub>
ClbK-C167A	c*c*agcaggtggcAGCactggcctgaaccgtcacgcaagggccggt aatattcaggcggtaagccagttgggacgtcaaatgatctttgt	Inactivation of ClbK-KS
ClbK-S747A	g*c*cgtaacgttgctgaatatcatataaaatggttgacgtaacagGGCa tgcccaccagttcgaagaagctggcgtggtgatcatcaat	Inactivation of ClbK-T <sub>1</sub>
ClbK-D939A	t*t*cccgaatgaacaactccagactccatgcacggctatcagcagAGC gatagatacatgtagccgggcttttctgctggatcaaccac	Inactivation of ClbK-Cy
ClbK-D944A	g*t*ggttgatccgcagcaaaaagcccggctacatgtatctatcgactgct gatagccGCCgcatggagctggagttgttcattcgggaa	Inactivation of ClbK-Cy
ClbK-D2	g*t*ggttgatccgcagcaaaaagcccggctacatgtatctatGCTctgc tgatagccGCCgcatggagctggagttgttcattcgggaa	Inactivation of ClbK-Cy
ClbK-R1768E	g*a*aatgacgatagctgcgTTCtttgatgtaacgtgtgctatccgccggt gcccgtcagtgcaatgccagaccatccagcgcgcaaatg	Inactivation of ClbK-Ox
ClbK-S1770E	g*g*tttttgcgcgctgaaatgacgataTTCggggcgtttgatgtaacgtg tgctatccggcgtgcccgtcagtgcaatgccagaccatc	Inactivation of ClbK-Ox
ClbK-2073A	c*c*cgataatgcctcaagtgcctgctgaatcgcaccaattctatAGCa ctgccccccagcgagaagaatcgtcttggccgacacgtg	Inactivation of ClbK-T <sub>2</sub>

ClbL-S179A	g*c*ggattcacccccgtggaattggcagcgatttgttggcGCCctgc gcattcccgcacactacacaggtgtctatgcccatcgtgt	Inactivation of ClbL-
ClbQ-S78A	g*t*gaacactacacaggtggagactacgccattttgggcatGCCctcg gagggatcatggccttcgaactggcattatattctgat	Inactivation of ClbQ-
ClbI-KS S178C	a*t*cgctatcacctcaacctgcgcggccggcgatcacggcagactt ccTGTtcgacatccttggtggcgggtgtgcgtggcatgcaa	Mutation of ClbI-KS active site to cysteine
ClbH-C2 H662A	g*a*tgacgatcgtagcgtattgttattGCgctgcaccacatcatcagtga tggtggcgaaggcgtttgttacgcgaattgcaggcc	Mutation of His near the active site in ClbH-C

\* = phosphorothioate linkage

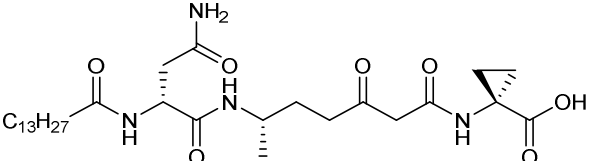
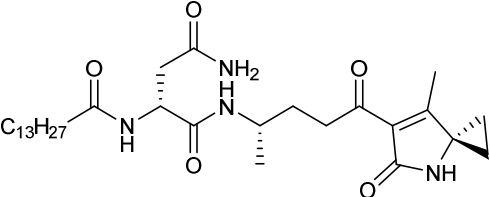
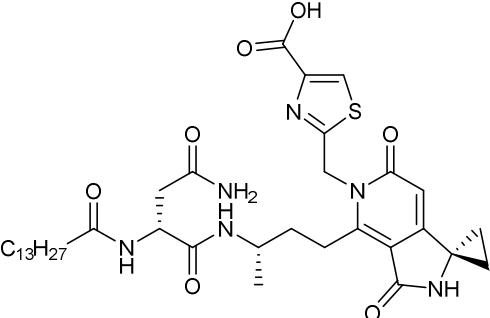
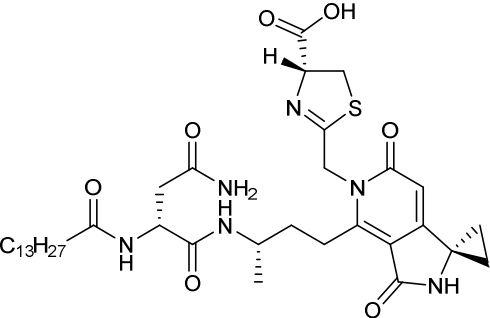
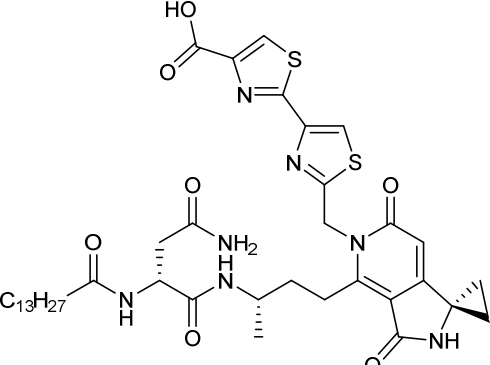
Screening Primers	Sequence	Purpose
wt-clb-f	ggtaaacgccttactcatcga	Forward primer for ClbP wild type screen
mut-clb-f	gtaaacgccttactcatcgc	Forward primer for ClbP S95A mutagenesis screen
clb-seq-rB	atgacaataatggaacacgtagc	Reverse primer for ClbP screens
A1-PCR_WT	CTGGCGTATATTATTACACCTCCGG	Forward primer for ClbH-A <sub>1</sub> wild type screen
A1-PCR_MU	AACTGGCGTATATTATTACACCTCCGA	Forward primer for ClbH-A <sub>1</sub> G162D mutagenesis screen
A1-PCR_REV	CTCCAGATACTCGACAAACAGGTTTCAG	Reverse primer for ClbH-A <sub>1</sub> screens
C-PCR_WT	GCGTATTGTTGATTCATCTGCACCA	Forward primer for ClbH-C wild type screen
C-PCR_MU	CGTATTGTTGATTCATCTGCACGC	Forward primer for ClbH-C H665A mutagenesis screen
C-PCR_REV	CATGTGTTGGCAGACAATGCG	Reverse primer for ClbH-C domain screens
C2-PCR_WT	ACGATCGTAGCGTATTGTTGATTCAT	Forward primer for noncatalytic His in ClbH-C wild type screen
C2-PCR_MU	GATCGTAGCGTATTGTTGATTGCG	Forward primer for noncatalytic His in ClbH-C H662A mutagenesis screen
A2-PCR_WT	CGGTGGTGATCTTTACCTCCGG	Forward primer for ClbH-A <sub>2</sub> wild type screen
A2-PCR_MU	CGGTGGTGATCTTTACCTCCGA	Forward primer for ClbH-A <sub>2</sub> G1137D mutagenesis screen
A2-PCR_REV	CACAGAGAGGCTGGCAGAAAGC	Reverse primer for ClbH-A <sub>2</sub> screens
T-PCR_WT	ATTTCTTCGATCTCGGTGGACACT	Forward primer for ClbH-T wild type screen
T-PCR_MU	TCTTCGATCTCGGTGGACACG	Forward primer for ClbH-T S1697A mutagenesis screen
T-PCR_REV	CAGTGATGACTGTCGGTTGTGGC	Reverse primer for ClbH-T mutagenesis screens
KS_WT	GATCACGGTGCAGACTTCCTCA	Forward primer for ClbI-KS mutations (WT rxns)
KS-A_MU	ACGGTGCAGACTTCGCG	Forward primer for ClbI-KS S178A mutation

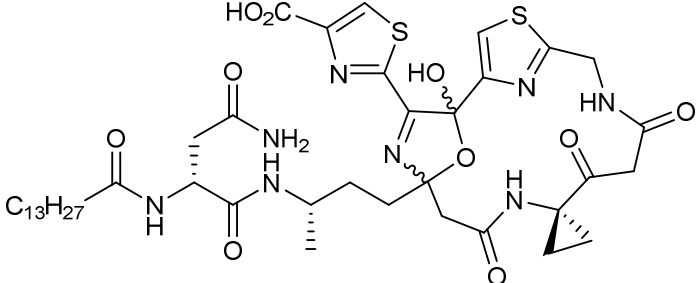
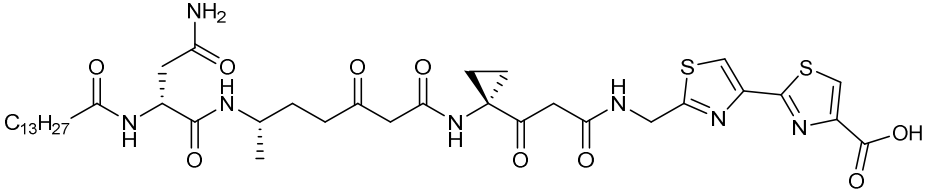
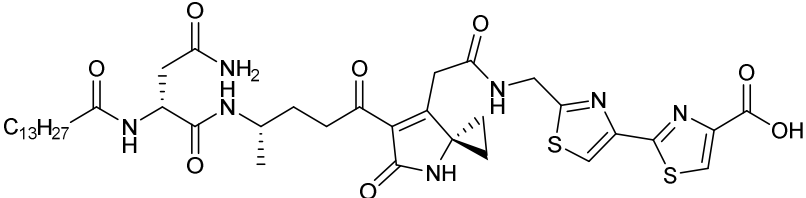
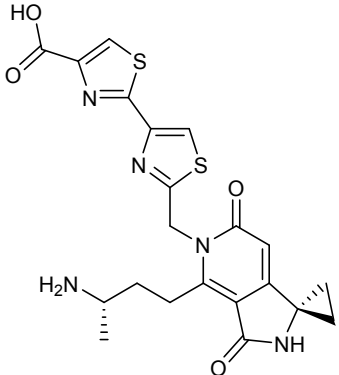
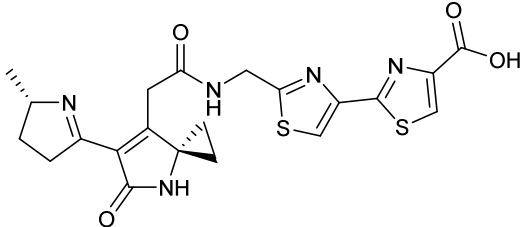
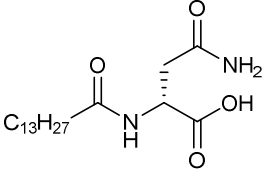
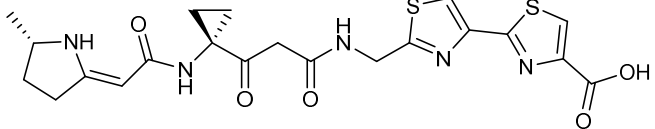
KS-C_MU	GATCACGGTGCAGACTTCCTGT	Forward primer for ClbI-KS S178C mutation
ClbI-KS_rev	TATAACTGATCTTCTCCGAACCGTCG	Reverse primer for ClbI-KS mutagenesis screen
ClbI-AT_WT	CCAACGGTAATGATTGGTCATTCG	Forward primer for ClbI-AT wild type screen
ClbI-AT_MU	CAACGGTAATGATTGGTCATGCC	Forward primer for ClbI-AT S625A mutagenesis screen
ClbI-AT_rev	CTTGCATCATGCTAGAGTGGAAGG	Reverse primer for ClbI-AT screens
ClbI-T_WT	CGAAGCTGGCGGACATTCA	Forward primer for ClbI-T wild type screen
ClbI-T_MU	GAAGCTGGCGGACATGCG	Forward primer for ClbI-T S952A mutagenesis screen
ClbI-T_rev	CCTGATTGCGCCAACGTGTCG	Reverse primer for ClbI-T screens
ClbJ-C_WT	GTAACGAGATACCGTCGATGATGATATG	Forward primer for ClbJ-C wild type screen
ClbJ-C_MU	GAGATACCGTCGATGATGATGGC	Forward primer for ClbJ-C H175A mutagenesis screen
ClbJ-C_rev	GTATCGTTTGCATGGCGTGGTG	Reverse primer for ClbJ-C screens
ClbJ-A1_WT	GCCTTTAGGTTACCGGTACTGC	Forward primer for ClbJ-A <sub>1</sub> wild type screen
ClbJ-A1_MU	ACGCCTTTAGGTTACCGGTACTAT	Forward primer for ClbJ- A <sub>1</sub> G650D mutagenesis screen
ClbJ-A1_rev	GATGCGTTTTTCGAGCGCATG	Reverse primer for ClbJ- A <sub>1</sub> screens
ClbJ-T1_WT	CGTTACCGCCAACAGCGA	Forward primer for ClbJ-T <sub>1</sub> wild type screen
ClbJ-T1_MU	AACGTTACCGCCAACAGTGC	Forward primer for ClbJ- T <sub>1</sub> S1033A mutagenesis screen
ClbJ-T1_rev	GAGCACCGTTACACAAAGCACTG	Reverse primer for ClbJ- T <sub>1</sub> screens
ClbJ-Cy_WT	AGAGCATCGGCAATCAGCAGAT	Forward primer for ClbJ-Cy D1226 screen
ClbJ-Cy_MU	GCATCGGCAATCAGCAGGG	Forward primer for ClbJ-Cy D1226A mutagenesis screen
ClbJ-Cy_rev	CGACCCACATCTACCATGAATTTG	Reverse primer for ClbJ-Cy screens
J1231A_WT	gtctcgatctgctgattgcccgat	Forward primer for ClbJ-Cy D1231 screen
J1231A_MU	CGATCTGCTGATTGCCGCC	Forward primer for ClbJ-Cy D1231A mutagenesis screen
ClbJ-A2_WT	CGGGGTACCGGTGGAGC	Forward primer for ClbJ-A <sub>2</sub> and ClbK-A wild type screens
ClbJ-A2_MU	TTCGGGGTACCGGTGGAAT	Forward primer for ClbJ-A <sub>2</sub> G1697D and ClbK-A G1411D mutagenesis screens
ClbJ-A2_rev	gggtaaatagttctctggcgctg	Reverse primer for ClbJ-A <sub>2</sub>

		screens
ClbJ-T2_WT	GCAACAGCACGATCTGGATTGA	Forward primer for ClbJ-T <sub>2</sub> wild type screen
ClbJ-T2_MU	CAACAGCACGATCTGGATGGC	Forward primer for ClbJ-T <sub>2</sub> S2095A mutagenesis screen
ClbJ-T2_rev	CAGAAAACCTGCATCCTGACGATAC	Reverse primer for ClbJ-T <sub>2</sub> screens
ClbK-KS_WT	CCACCAGCGAGGTGGCACA	Forward primer for ClbK-KS wild type screen
ClbK-KS_MU	CCACCAGCGAGGTGGCAGC	Forward primer for ClbK-KS C167A mutagenesis screen
ClbK-KS_rev	gctacagccgtgcagaagcag	Reverse primer for ClbK-KS screens
ClbK-T1_WT	CATATAAAATGGTTGACGCTAACAGCGA	Forward primer for ClbK-T <sub>1</sub> wild type screen
ClbK-T1_MU	CATATAAAATGGTTGACGCTAACAGGGC	Forward primer for ClbK-T <sub>1</sub> S747A mutagenesis screen
ClbK-T1_rev	cccgatgtctgctctttgatgct	Reverse primer for ClbK-T <sub>1</sub> screens
ClbK-Cy_WT	TGCATCGGCTATCAGCAGGT	Forward primer for ClbK-Cy D939 wild type screen
ClbK-Cy_MU	ATGCATCGGCTATCAGCAGAG	Forward primer for ClbK-Cy D939A mutagenesis screen
ClbK-Cy_rev	CCACCCATATCTATGTGGAATATGAAC	Reverse primer for ClbK-Cy screens
K944_WT	GTATCTATCGACCTGCTGATAGCCGAT	Forward primer for ClbK-Cy D944 wild type screen
K944_MU	TCGACCTGCTGATAGCCGCC	Forward primer for ClbK-Cy D944 mutagenesis screen
ClbK-A_rev	CTCAAGATGTGCTGGCGCTG	Reverse primer for ClbK-A G1411D screens
ClbK-OXr_WT	AATGACGATAGCTGCGGCG	Forward primer for ClbK-OX R1768 wild type screen
ClbK-OXr_MU	CGAATGACGATAGCTGCGTTC	Forward primer for ClbK-OX R1768E mutagenesis screen
ClbK-OX_rev	GAATGGTTACCGTATCGAACTGGG	Reverse primer for ClbK-OX screens
ClbK-OXs_WT	CGCGCTGAAATGACGATAGCT	Forward primer for ClbK-OX S1770 wild type screen
ClbK-OXs_MU	GCGCGCTGAAATGACGATATTC	Forward primer for ClbK-OX S1770E mutagenesis screen
ClbK-T2_WT	CCTGCTGAATACGCACCAATTCTATAGA	Forward primer for ClbK-T <sub>2</sub> wild type screen
ClbK-T2_MU	CTGCTGAATACGCACCAATTCTATAGC	Forward primer for ClbK-T <sub>2</sub> S2073A mutagenesis screen
ClbK-T2_rev	GAGAAACCGAAGGAAACCGCTG	Reverse primer for ClbK-T <sub>2</sub> screens
L179-WT	GGCAGCGATTTGTTTGGCTCA	Forward primer for ClbL wild type screen
L179-MU	CAGCGATTTGTTTGGCGCC	Forward primer for ClbL

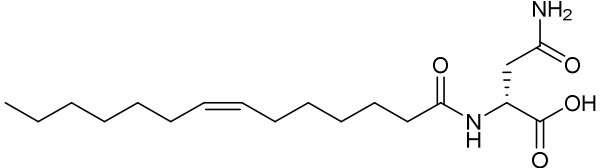
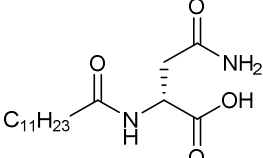
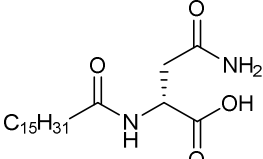
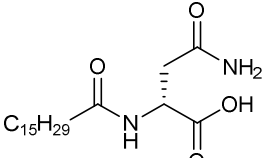
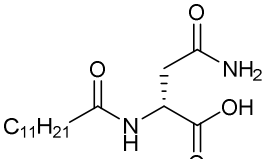
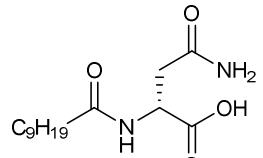
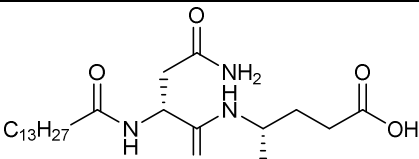
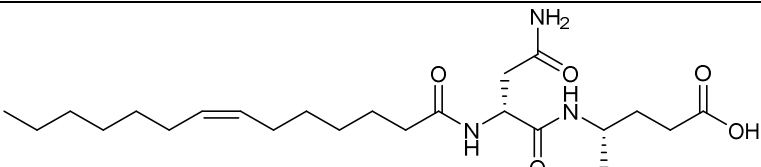
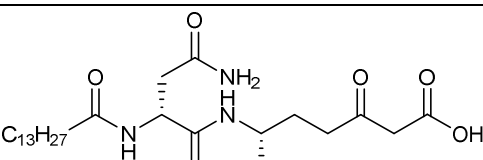
		S179A mutagenesis screen
L179-rev	CGCTGTGCGATCTGTTGATCTATCTC	Reverse primer for ClbL screens
Q78-WT	GAGACTACGCCATTTTTGGGCATAGT	Forward primer for ClbQ wild type screen
Q78-MU	CGCCATTTTTGGGCATGCC	Forward primer for ClbQ S78A mutagenesis screen
Q78-rev	CACGATCGGACAGGTTAATGTGC	Reverse primer for ClbQ screens
prPE141	GTCCGACAGCACGCTACGC	forward primer for <i>clbP</i> overspanning PCR
prPE142	CAAATCAGCGACACTGAATAC	reverse primer for <i>clbP</i> overspanning PCR
clbH-5P	gtaaaaaattacatgtctgaacagcaaggattatgagacagttg	Forward primer for <i>clbH</i> overspanning PCR
ClbH-3E	gtaaaaaattgaattcttagtggtggtggtggtggtgatgactg tcggtgtggtgc	Reverse primer for <i>clbH</i> overspanning PCR
pEClbI-NdeI-5'	gtaaaatCATATGGCAGAGAATGATTTTGGT ATAGCTATC	Forward primer for <i>clbI</i> overspanning PCR
pEClbI-AatII-3'	gtaaaatGACGTCTCATTTTTCAAACGCGG ATGGCTCCAGCCGCCCTCATTAATCATG TCGTAACTAGCACGG	Reverse primer for <i>clbI</i> overspanning PCR
ClbJ-5'	ATGACGATACATCATGCCGCATTG	Forward primer for <i>clbJ</i> overspanning PCR
ClbJ-3'	TTAACGCTGACGCTGGTGACG	Reverse primer for <i>clbJ</i> overspanning PCR
ClbK-5'_2	CGTCACCAGCGTCAGCGTTAAG	Forward primer for <i>clbK</i> overspanning PCR
ClbK-3'_2	GTCCCTGCGCTACGATAGCTCTG	Reverse primer for <i>clbK</i> overspanning PCR
ClbL-5'	gtaaaaaatGCTAGCAAGAAGGAGATATACCA TGAGTGAGCAGAGCTATCGTAGCG	Forward primer for <i>clbL</i> overspanning PCR
ClbL-3'	gtaaaaaatTCTAGACTAGTACCCTTCCGGTAC CGTGAATC	Reverse primer for <i>clbL</i> overspanning PCR
clbQ-5	gtaaaaaattcatatgagtaatatcagtttgattgttgccatattc	Forward primer for <i>clbQ</i> overspanning PCR
ClbQ-3	gtaaaaaattctcgagttagtggtggtggtggtggtgcctactatt cgagtgattcaatcgtct	Reverse primer for <i>clbQ</i> overspanning PCR
clbO-KO5	gactataaacacgatgccaacccttaaggaataacaacatgtag gctggagctgcttc	Forward primer for <i>clbO</i> deletion
clbO-KO3	ccattattgtcatctgtgaacacctataaaataccatcattccggg gatccgctgacc	Reverse primer for <i>clbO</i> deletion
clbO-S5	agttaaatattgcgcgctcggc	Forward primer for <i>clbO</i> overspanning PCR
clbO-S3	acacttacggaaagggtgggac	Reverse primer for <i>clbO</i> overspanning PCR

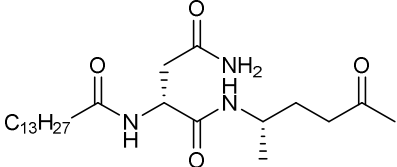
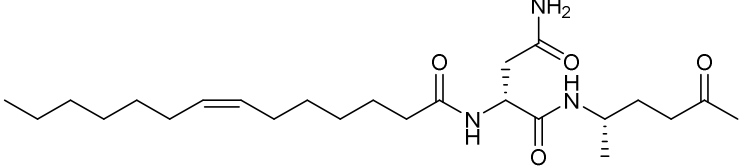
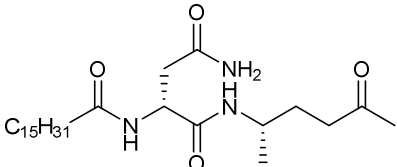
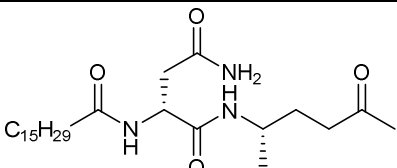
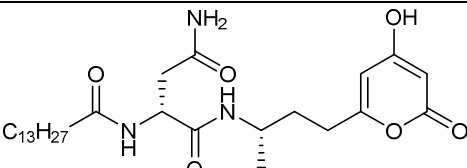
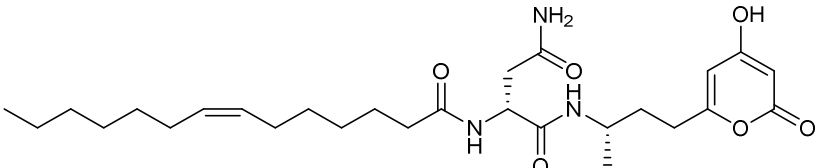
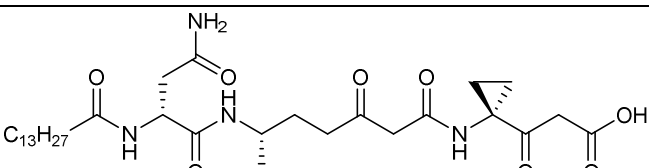
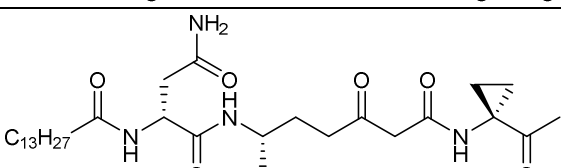
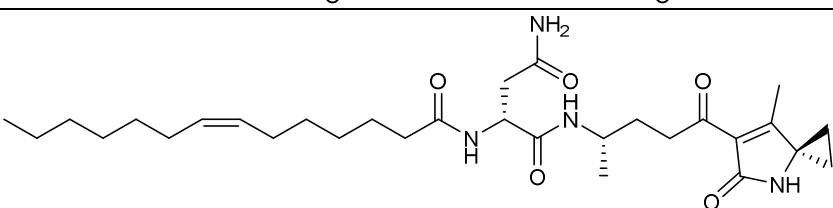
**Table S3. Known colibactin-dependent metabolites**

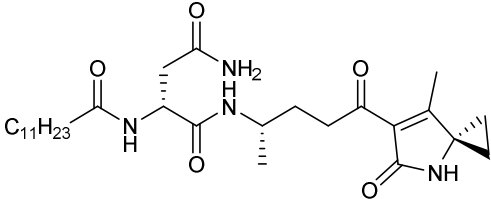
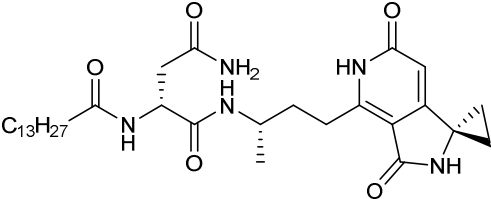
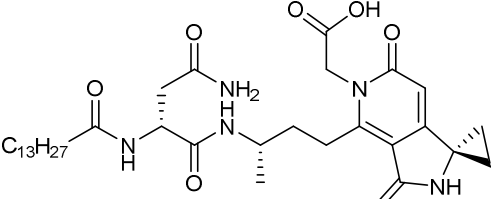
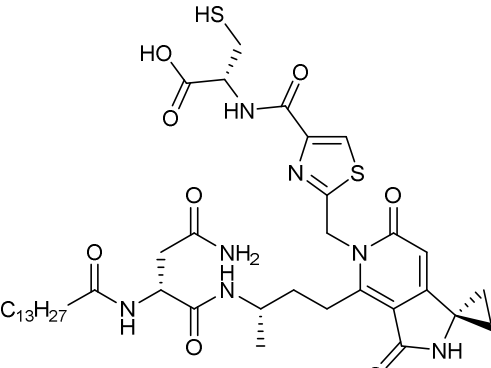
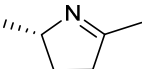
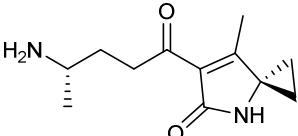
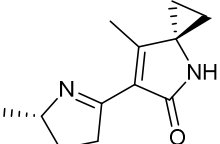
Neutral Mass	Structure	Reference
<p><b>1</b> 566.3679</p>		<p>12</p>
<p><b>2</b> 546.3781</p>		<p>12-13</p>
<p><b>3</b> 712.3618</p>		<p>7, 14</p>
<p><b>4</b> 714.3775</p>		<p>This study</p>
<p><b>5</b> 795.3448</p>		<p>7, 13b, 14</p>

<p><b>6</b> 886.3717</p>		<p>Structure - 15 Labeling - 12, 15</p>
<p><b>7</b> 831.3659</p>		<p>This study</p>
<p><b>8</b> 813.3554</p>		<p>This study</p>
<p><b>9</b> 471.1035</p>		<p>MS - 7, Structure - This study</p>
<p><b>10</b> 471.1035</p>		<p>This study</p>
<p><b>11</b> 342.2519</p>		<p>11, 16</p>
<p><b>12</b> 489.1141</p>		<p>This study</p>



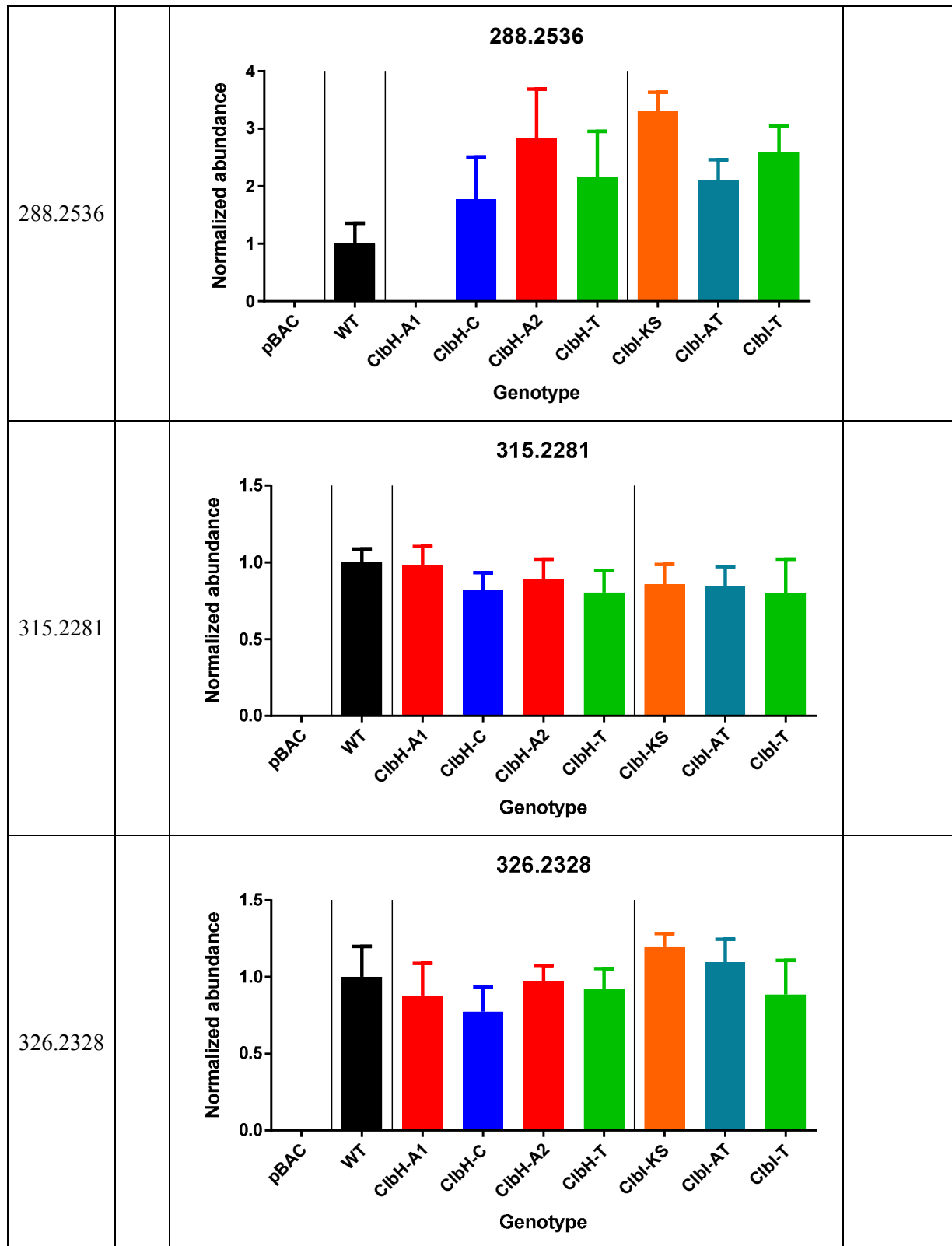
<p><b>S3</b> 340.2362</p>		<p>11</p>
<p><b>S4</b> 314.2206</p>		<p>11, 17</p>
<p><b>S5</b> 370.2832</p>		<p>11, 16b</p>
<p><b>S6</b> 368.2675</p>		<p>11, 16b</p>
<p><b>S7</b> 312.2049</p>		<p>17</p>
<p><b>S8</b> 286.1893</p>		<p>17</p>
<p><b>S9</b> 441.3203</p>		<p>11, 13a</p>
<p><b>S10</b> 439.3046</p>		<p>12</p>
<p><b>S11</b> 483.3308</p>		<p>11</p>

<p><b>S12</b> 439.3410</p>		<p>11</p>
<p><b>S13</b> 437.3254</p>		<p>12</p>
<p><b>S14</b> 467.3723</p>		<p>12</p>
<p><b>S15</b> 465.3567</p>		<p>12</p>
<p><b>S16</b> 507.3308</p>		<p>12</p>
<p><b>S17</b> 505.3152</p>		<p>12</p>
<p><b>S18</b> 608.3785</p>		<p>12</p>
<p><b>S19</b> 564.3887</p>		<p>14</p>
<p><b>S20</b> 544.3625</p>		<p>12</p>

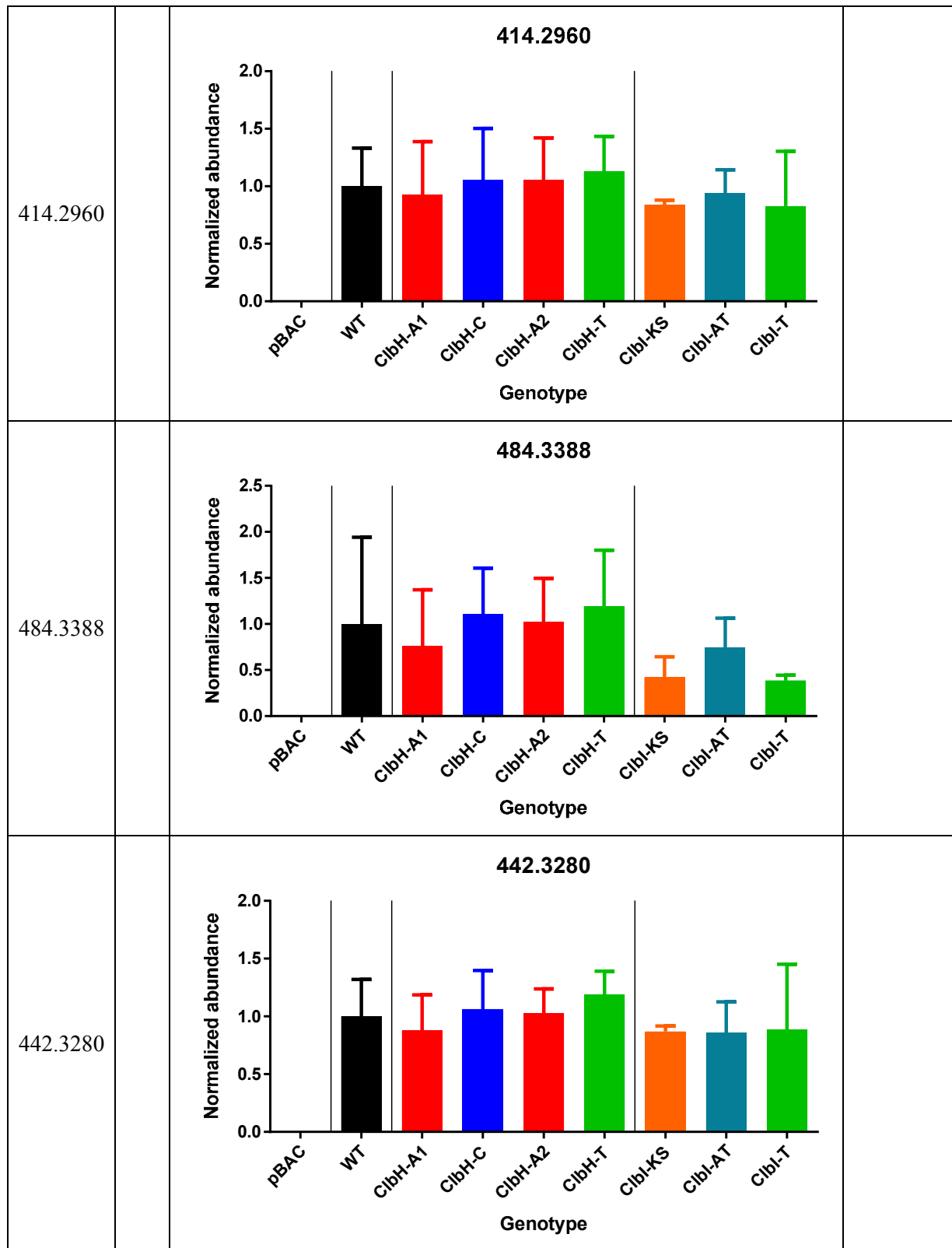
<p><b>S21</b> 518.3468</p>		<p>12</p>
<p><b>S22</b> 571.3734</p>		<p>14</p>
<p><b>S23</b> 629.3788</p>		
<p><b>S24</b> 815.3710</p>		<p>7</p>
<p><b>S25</b> 97.0891</p>		<p>11</p>
<p><b>S26</b> 222.1368</p>		<p>12, this study</p>
<p><b>S27</b> 204.1263</p>		<p>12, this study</p>

**Table S4. Multidomain signatures of colbactin-dependent metabolites in a wild-type ClbP background**

<i>m/z</i>	RT	Multidomain signature	Structure
205.1338	0.9	<p style="text-align: center;"><b>205.1338</b></p> <p style="text-align: center;">Normalized abundance</p> <p style="text-align: center;">Genotype</p>	S27
223.1444	0.9	<p style="text-align: center;"><b>223.1444</b></p> <p style="text-align: center;">Normalized abundance</p> <p style="text-align: center;">Genotype</p>	S26
260.2223		<p style="text-align: center;"><b>260.2223</b></p> <p style="text-align: center;">Normalized abundance</p> <p style="text-align: center;">Genotype</p>	



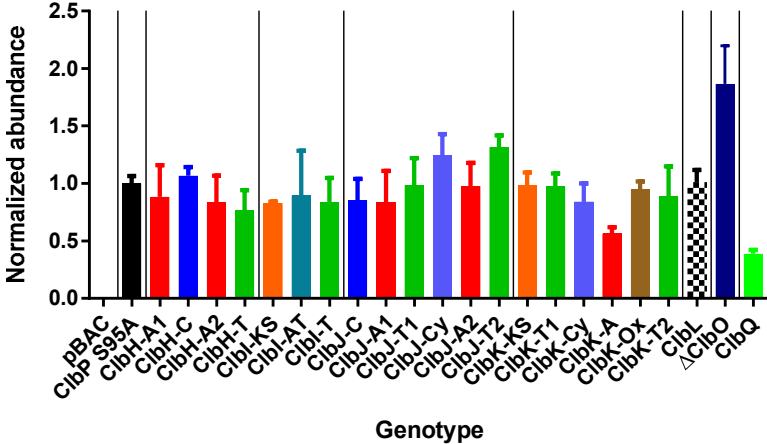
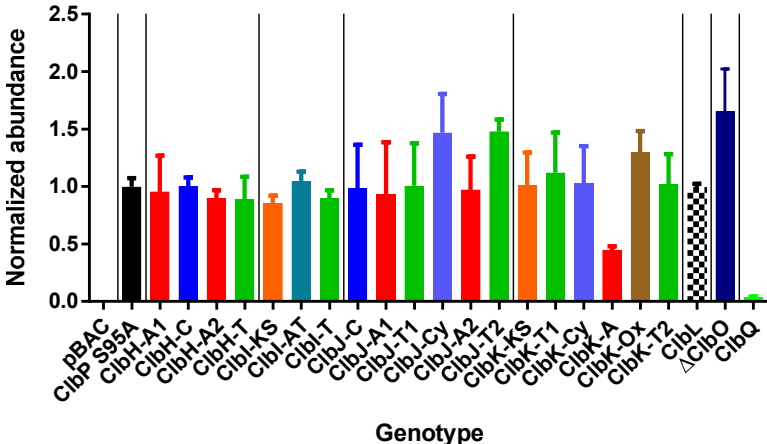
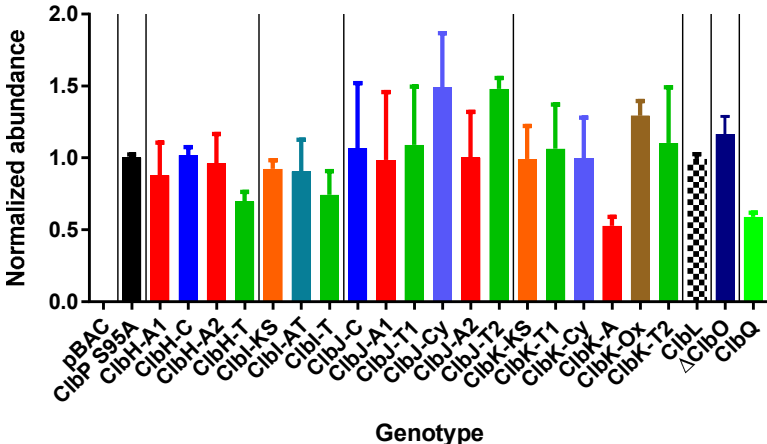
341.2440	<p style="text-align: center;"><b>341.2440</b></p> <p style="text-align: center;">Normalized abundance</p> <p style="text-align: center;">Genotype</p>	
343.2592	<p style="text-align: center;"><b>343.2592</b></p> <p style="text-align: center;">Normalized abundance</p> <p style="text-align: center;">Genotype</p>	S1
369.3748	<p style="text-align: center;"><b>369.3748</b></p> <p style="text-align: center;">Normalized abundance</p> <p style="text-align: center;">Genotype</p>	



**Table S5. Multidomain signatures of colbacin-dependent metabolites in a C1bP S95A background**

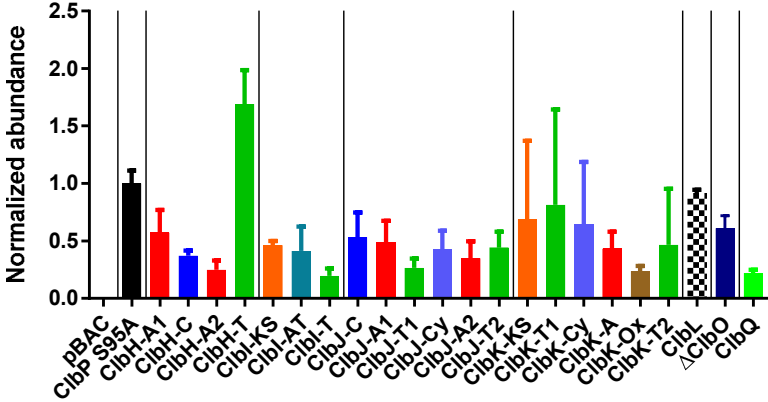
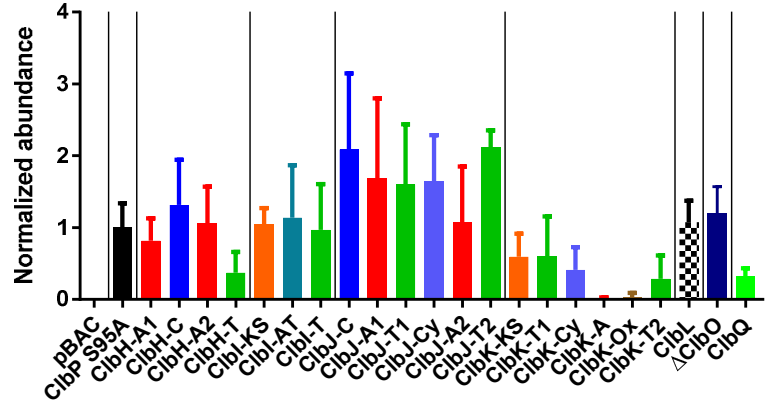
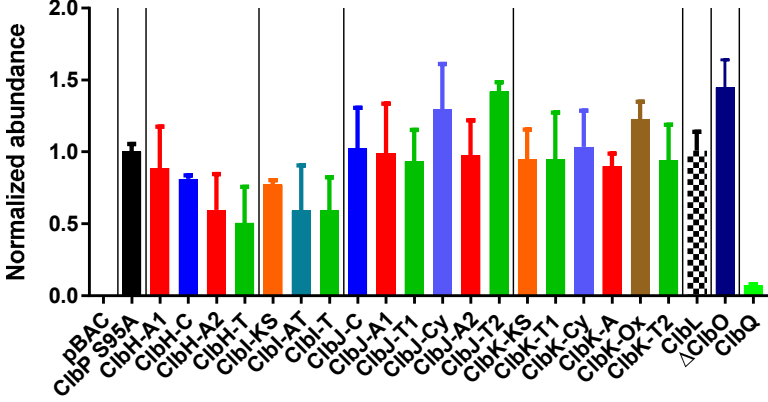
<i>m/z</i>	RT	Multidomain signature	Structure
343.2592	16.9	<p style="text-align: center;"><b>343.2592</b></p> <p style="text-align: center;">Normalized abundance</p> <p style="text-align: center;">Genotype</p>	11
386.2650	14.3	<p style="text-align: center;"><b>386.2650</b></p> <p style="text-align: center;">Normalized abundance</p> <p style="text-align: center;">Genotype</p>	
412.2806	15.2	<p style="text-align: center;"><b>412.2806</b></p> <p style="text-align: center;">Normalized abundance</p> <p style="text-align: center;">Genotype</p>	



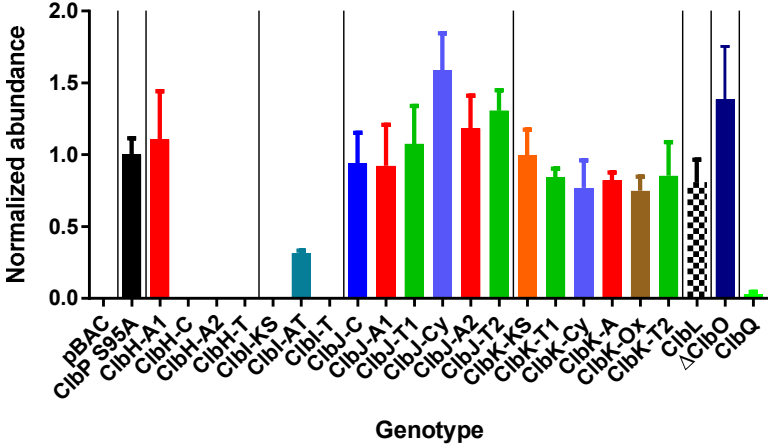
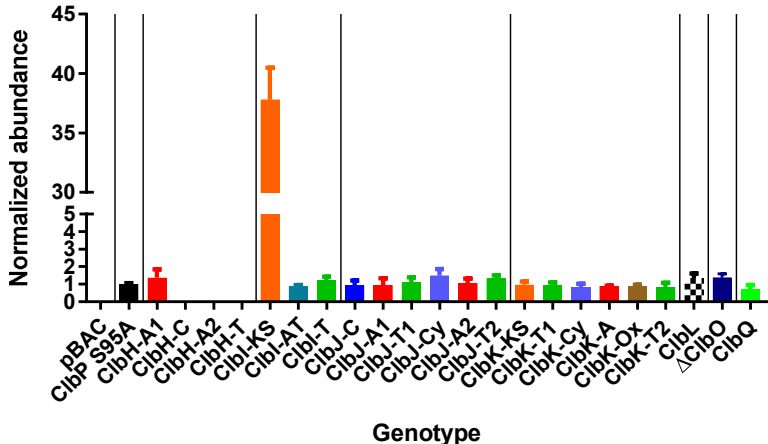
412.3168	17.5	<p style="text-align: center;"><b>412.3168</b></p>  <p style="text-align: center;"><b>Genotype</b></p>	
414.2960	14.5	<p style="text-align: center;"><b>414.2960</b></p>  <p style="text-align: center;"><b>Genotype</b></p>	
414.2960	16.4	<p style="text-align: center;"><b>414.2960</b></p>  <p style="text-align: center;"><b>Genotype</b></p>	

434.2991	15.5	<p style="text-align: center;"><b>434.2991</b></p> <p style="text-align: center;">Normalized abundance</p> <p style="text-align: center;">Genotype</p>	
438.3326	16.4	<p style="text-align: center;"><b>438.3326</b></p> <p style="text-align: center;">Normalized abundance</p> <p style="text-align: center;">Genotype</p>	
440.3485	17.7	<p style="text-align: center;"><b>440.3485</b></p> <p style="text-align: center;">Normalized abundance</p> <p style="text-align: center;">Genotype</p>	S12

442.3280	16.6	<p style="text-align: center;"><b>442.3280</b></p> <p style="text-align: center;">Normalized abundance</p> <p style="text-align: center;">Genotype</p>	S9
466.3650	18.4	<p style="text-align: center;"><b>466.365</b></p> <p style="text-align: center;">Normalized abundance</p> <p style="text-align: center;">Genotype</p>	S15
468.3791	18.6	<p style="text-align: center;"><b>468.3791</b></p> <p style="text-align: center;">Normalized abundance</p> <p style="text-align: center;">Genotype</p>	S14

480.3069	14.7	<p style="text-align: center;"><b>480.3069</b></p>  <p style="text-align: center;">Normalized abundance</p> <p style="text-align: center;">Genotype</p>	
484.3388	16.7	<p style="text-align: center;"><b>484.3388</b></p>  <p style="text-align: center;">Normalized abundance</p> <p style="text-align: center;">Genotype</p>	S11
486.3538	15.9	<p style="text-align: center;"><b>486.3538</b></p>  <p style="text-align: center;">Normalized abundance</p> <p style="text-align: center;">Genotype</p>	

519.3539	15.4	<p style="text-align: center;"><b>519.3539</b></p> <p style="text-align: center;">Normalized abundance</p> <p style="text-align: center;">Genotype</p>	S21
545.3696	16.2	<p style="text-align: center;"><b>545.3696</b></p> <p style="text-align: center;">Normalized abundance</p> <p style="text-align: center;">Genotype</p>	S20
547.3854	17.4	<p style="text-align: center;"><b>547.3854</b></p> <p style="text-align: center;">Normalized abundance</p> <p style="text-align: center;">Genotype</p>	2

563.3796	15.7	<p style="text-align: center;"><b>563.3796</b></p>  <p style="text-align: center;">Normalized abundance</p> <p style="text-align: center;">Genotype</p>	
565.3960	16.9	<p style="text-align: center;"><b>565.3960</b></p>  <p style="text-align: center;">Normalized abundance</p> <p style="text-align: center;">Genotype</p>	S19
567.3752	16.7	<p style="text-align: center;"><b>567.3752</b></p>  <p style="text-align: center;">Normalized abundance</p> <p style="text-align: center;">Genotype</p>	1

573.3646	17.2	<p style="text-align: center;"><b>573.3646</b></p> <p style="text-align: center;"><b>Normalized abundance</b></p> <p style="text-align: center;"><b>Genotype</b></p>	
609.3858	16.4	<p style="text-align: center;"><b>609.3858</b></p> <p style="text-align: center;"><b>Normalized abundance</b></p> <p style="text-align: center;"><b>Genotype</b></p>	<b>S18</b>
630.3861*	15.7	<p style="text-align: center;"><b>630.3861</b></p> <p style="text-align: center;"><b>Normalized abundance</b></p> <p style="text-align: center;"><b>Genotype</b></p>	

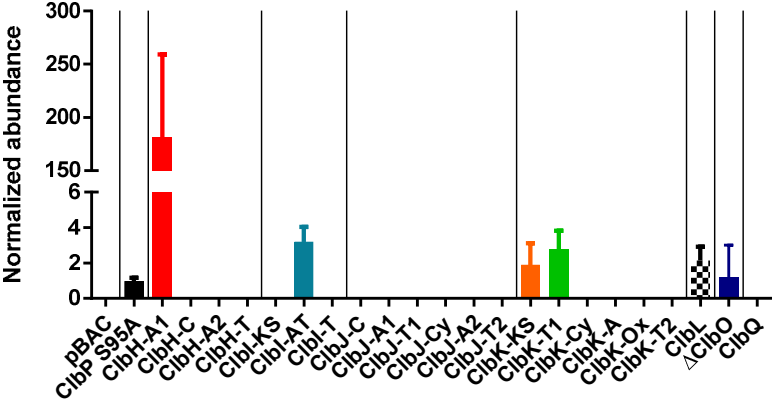
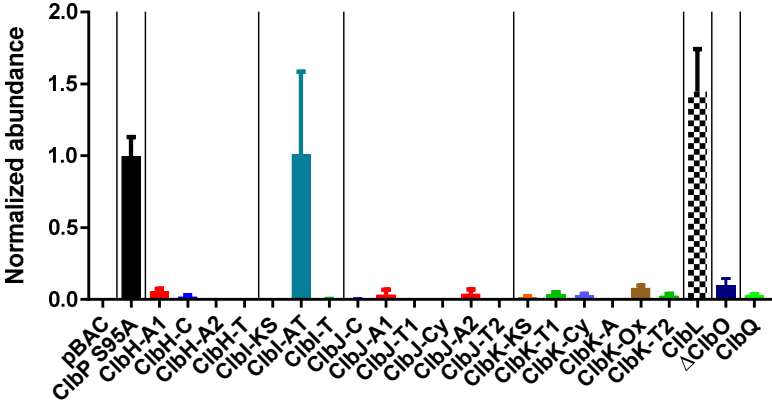
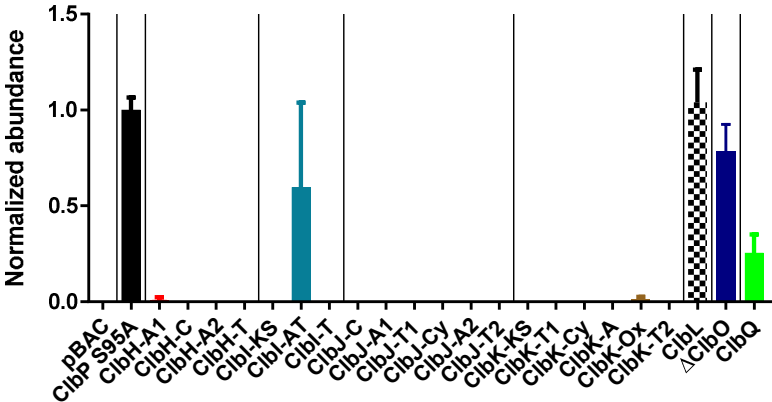
648.3967*	15.5	<p style="text-align: center;"><b>648.3967</b></p> <p style="text-align: center;">Normalized abundance</p> <p style="text-align: center;">Genotype</p>	
711.3534	15.2	<p style="text-align: center;"><b>711.3534</b></p> <p style="text-align: center;">Normalized abundance</p> <p style="text-align: center;">Genotype</p>	
713.3691	16.2	<p style="text-align: center;"><b>713.3691</b></p> <p style="text-align: center;">Normalized abundance</p> <p style="text-align: center;">Genotype</p>	3

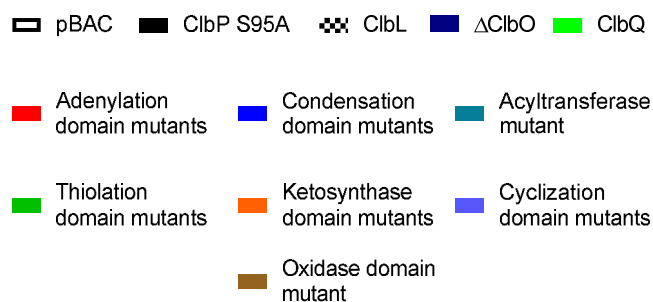
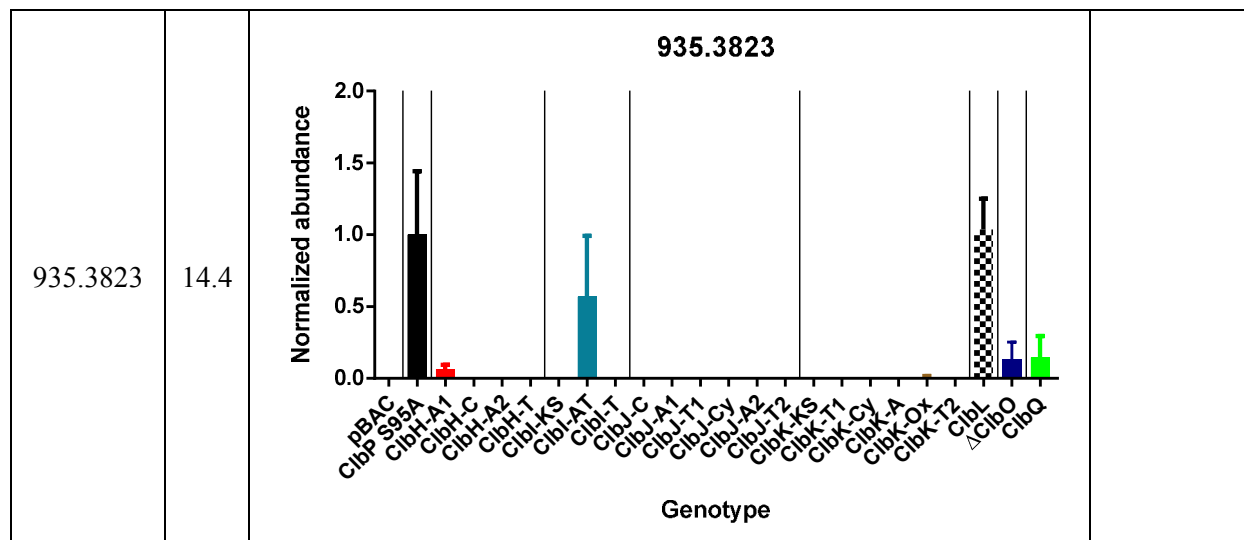


715.3847*	16.2	<p style="text-align: center;"><b>715.3847</b></p> <p style="text-align: center;"><b>Normalized abundance</b></p> <p style="text-align: center;"><b>Genotype</b></p>	4
731.3797*	15.5	<p style="text-align: center;"><b>731.3797</b></p> <p style="text-align: center;"><b>Normalized abundance</b></p> <p style="text-align: center;"><b>Genotype</b></p>	
733.3953*	16.0	<p style="text-align: center;"><b>733.3953</b></p> <p style="text-align: center;"><b>Normalized abundance</b></p> <p style="text-align: center;"><b>Genotype</b></p>	

733.3953*	16.2	<p style="text-align: center;"><b>733.3953</b></p> <p style="text-align: center;">Normalized abundance</p> <p style="text-align: center;">Genotype</p>	
749.3906	15.9	<p style="text-align: center;"><b>749.3906</b></p> <p style="text-align: center;">Normalized abundance</p> <p style="text-align: center;">Genotype</p>	
796.3521	16.1	<p style="text-align: center;"><b>796.3521</b></p> <p style="text-align: center;">Normalized abundance</p> <p style="text-align: center;">Genotype</p>	5

814.3573*	15.6	<p style="text-align: center;"><b>814.3626</b></p> <p style="text-align: center;"><b>Genotype</b></p>	
814.3573*	16.0	<p style="text-align: center;"><b>814.3626</b></p> <p style="text-align: center;"><b>Genotype</b></p>	8
816.3783	16.7	<p style="text-align: center;"><b>816.3783</b></p> <p style="text-align: center;"><b>Genotype</b></p>	S24

832.3732*	16.2	<p style="text-align: center;"><b>832.3732</b></p>  <p style="text-align: center;">Normalized abundance</p> <p style="text-align: center;">Genotype</p>	7
852.3859*	15.3	<p style="text-align: center;"><b>852.3859</b></p>  <p style="text-align: center;">Normalized abundance</p> <p style="text-align: center;">Genotype</p>	
887.3796	15.9	<p style="text-align: center;"><b>887.3796</b></p>  <p style="text-align: center;">Normalized abundance</p> <p style="text-align: center;">Genotype</p>	6



New ions are indicated with an asterisk

## Supplemental Figures

### A. Ketosynthase domains

```

130          140          150          160          170*
ClbB SPHWLN.AVMQDT.TDSTALYKASILNIHSVTA.LIAHA*LNLTC*CPAVTLDTA*CSTSAVAI
ClbC DVDWLRRSLSQIG.GDALNRFESGIYGHKDLLAHLIAYS*LNLNCPVYSLYTSCSTSLSAT
ClbI DSYLMNLNMPHFKRVFSSGSLQAAIIGNDKDSITTTIAYH*LNLRC*CPAIVTQTS*SSTSLVAV
ClbK SFYLLTHLMNPPDKLAQLGGLOIMVGN*DKHLLTSQIAYRLNIT*CPCVTVQAS*CATSLVAV
ClbO NNYFIDR*VYPYLKMSGDHHYLAQIGNEKDYLCQAQVAYKLGFT*CPAVSVQTA*CSSSLVAA

```

### B. Thiolation domains

```

1 10 20 30* 40 50 60
clbJ-T2 .....QQVAALWCEVLRQREQIGLNDNFFEAG.GGSIQIVLLHRRIEEIFKVTVP*IAELFRL..TVKRR
clbK-T2 .....QRLVALWQEVLRGVSHVSAEDDFFSLG.GSSELVRIQQALEAIIQOEIP*IVDLFRL..PTIAD
ClbH .....ORLAEIQWQLRGLERVTGTTNFFDLG.GHSLLLVQMQQYIGQQCGQHVAVLDLLRF..TTIKR
clbB-T1 .....HALHAIWQRVLRDQDIDSNASFFALG.GTSLDTIRVKGDIKRLGLEIDITDLFKY..PTLTA
clbB-T2 .....RVLCQILEEYLRGLDRVGIDDN*YAEELG.ATSLDMVQLSGQMARHYP.QVSVVSLYNH..ATVRQ
ClbI .....RGLVAICEALLGIDGLGIDDNFFEAG.GHSLMLGMLLAQVQERFAVTLSFFDV*MED..ASVRA
clbJ-T1 .....LLALWMRYLPIKNVDPECDFFRLG.GHSLLA*AVTLVAEINRTFHCALTKKIFHY..STLRA
clbK-T1 .....AVVTEI*WERTLRGVSIDDHNASFFELG.GHSLLASTILYDIQQRYGITCTLSAFFAD..PTIEG
clbc-T .....QYITCLMELLLEISPVGVDDDFFELG.GHSLLV*TQLTSRLERDFNVHIDL*LLTLMEN..PNPRN
clbO-T VSYLSVSDVEK*TWRSLRCIDHYDEHAVIFEY*G.ATSMHVISFVDSCHNIYKIGLTAAD*IYAR..PAIRE
ClbE MKKQDMKAAIREFLSRSLRGHTLNDDDH*IFSLGLVHSLFTVQIILFIEKNFQVELE*SELKTEQIATV*NK
clbN-T .....VRVCVEGAL*LEQTEFDDNENLYVVLG.LD*SHKSIQIAAQLR.HHGWTMSAVQVMEC..GTVNA

```

### C. Condensation domains

```

110 120 130 * 140 150
ClbH PLTSGTPLCRF.EL*LTLD*DDR*SVLLIHH*IISDC*WSKGVLLRE*LQAAYN.....
ClbJ_1 DLARG.PLWGV.TQIIQ..PDQGCHLVFC*ARR*IIDG*ISLRL*LFDEL*LQQQYARLHAG...
ClbB KYPESLKTIPVRAYLIQ..STKESAFILSYHH*IVMDG*WSLSLF*IKQL*LLQLYGA*AVVSGVR
ClbN RQPF*TLLA*HDL*FEFV*TFTCGEQYSGYLFK*ARR*GIADG*WSMALL*SNHV*KRAYE.....

```

### D. Cyclization domains

```

120 130 * 140 150 160 170
ClbJ_2 ACTA*QHGR*RLH*FS*EDLLI*ADAL*SMRTLQQEL*MMLYR*EP*HVS*LP*LP*FS*FRDYV*QAL*LVEQA
ClbK VDPQ*QKAR*RLH*V*S*EDLLI*ADAW*SELFIR*ELAY*HYR*HP*QAA*LP*LT*YS*FRDYV*LT*LKSYEK

```

### E. Adenylation domains

```

120 130 * 140 150 160 170
ClbJ-A2 LPEVAGDVT*D.LAYIIFTSC*STGTPKGV*MIDHRAAMNTLED*INERFGLNAQDRV*FGLSS*L
ClbK-A LPEVAGDVT*D.LAYIIFTSC*STGTPKGV*MIDHRAAMNTLED*INERFGLNAQDRV*FGLSS*L
ClbN-A EPWPAIEPQD.LAYVLF*TSC*STGTPKGV*QVSHGNLANYLHFAAERY.FTAQDR*AAALYSS*L
ClbH-A2 PVSVA*PDALDCDA*VVIFTSC*TGTPKGV*RLSQRN*LVNLTASFISSYQVTHQD*VLLPIT*SV
ClbJ-A1 YSTPCALLPDMQAYLL*F*TSC*STGTPKGV*CVVHRG*LLNLLDMQRTFAVGSQD*RLLSV*ITP
ClbH-A1 DLRYRPHARQ.LAYIIYTSC*STGTPKGV*VATEHAA*LLN*RIVW*QONAYP*ISSQD*VLFQKT*VY
ClbB-A SVVFPVITPDSRAYVIYSS*STGTPKGV*I*AVHRG*LLRLIQ.GDSPLK*VESGET*TLT*CPF

```

**Figure S1. Protein sequence alignments of NRPS-PKS domains from the colibactin pathway.** The sites selected for mutation are denoted with an asterisk. **(A)** The ketosynthase active site is a conserved cysteine residue; however, in ClbI, the active site is naturally mutated to serine. **(B)** The phosphopantetheine attachment site of thiolation domains is a conserved serine residue; mutation to alanine abolishes activity by preventing posttranslational modification. **(C)** The second histidine in the HHxxxDG motif of condensation domains acts as a catalytic base; mutation to alanine abolishes activity. **(D)** The DxxxxD motif of cyclization domains was previously thought to act as the catalytic base in the cyclization reactions. While this has recently been shown to be structurally inaccurate, mutation of both aspartates to alanine abolishes activity *in vivo*. **(E)** Adenylation domains contain a flexible loop that interacts with the pyrophosphate leaving group upon adenylation. Mutation of the glycine in this loop to aspartate abolishes activity.

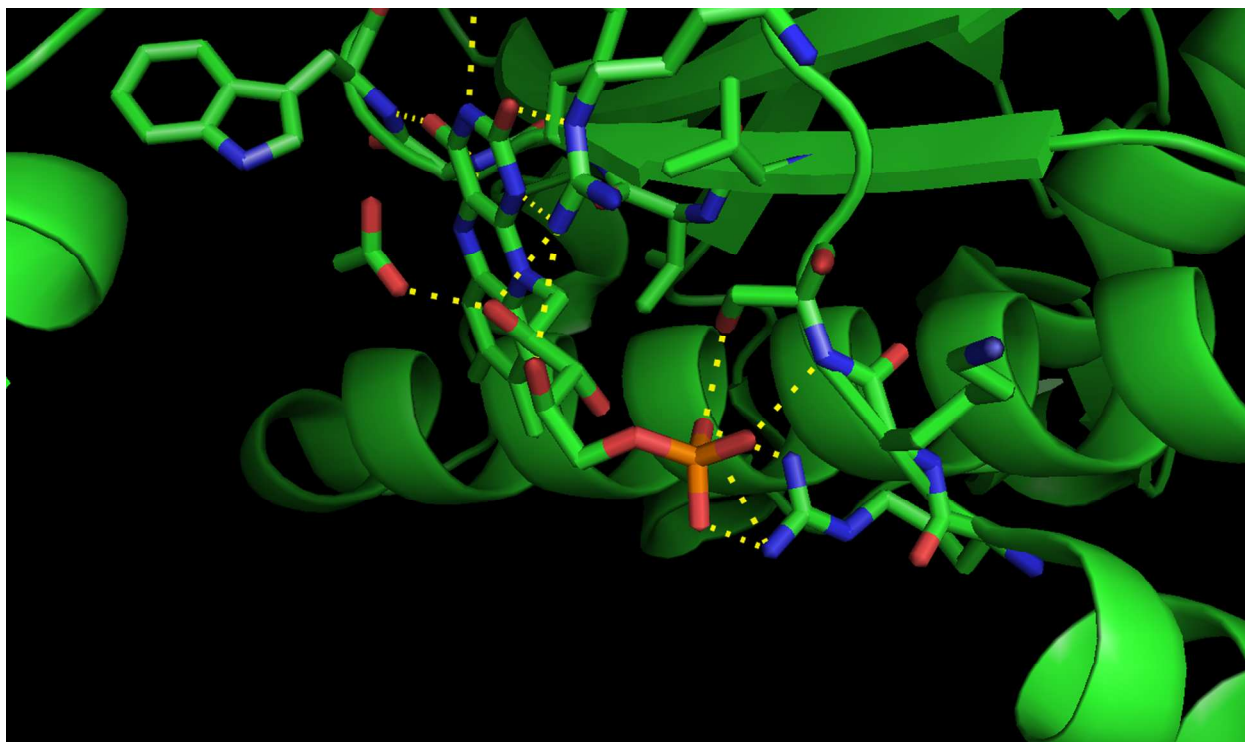
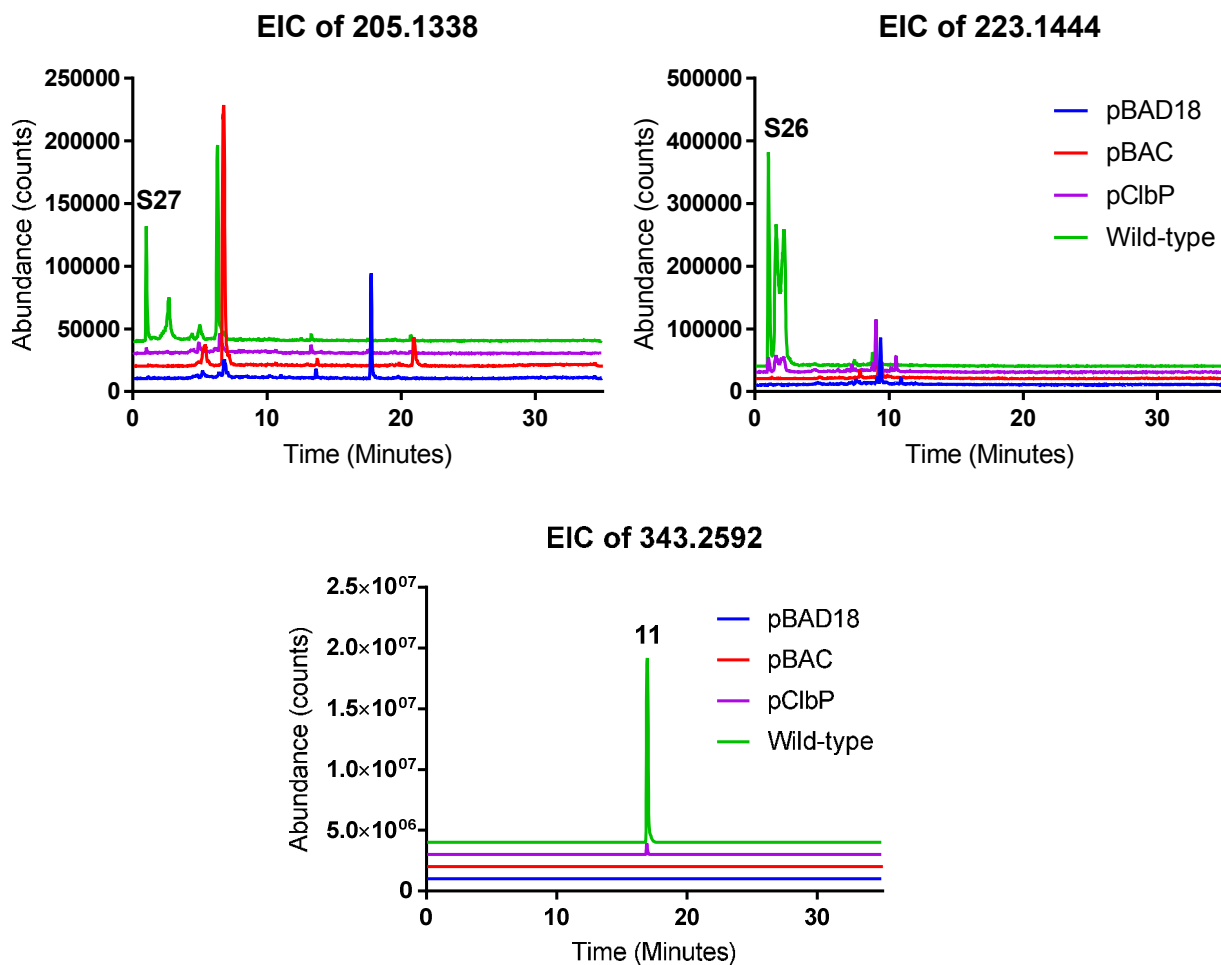


**Figure S2. FMN-binding site of the ClbK oxidase domain homolog from *Ralstonia eutropha*** (PDB code: 3hj9). Hydrogen bonds, depicted by yellow dashes, identify residues to mutate to disrupt the flavin mononucleotide (FMN)-binding site. Residues R1768 and S1770 hydrogen bond with the phosphate of FMN and are conserved across the mcbC-like oxidoreductase family. These residues were mutated to aspartate residues to introduce a repulsive electrostatic interaction, which abolished activity *in vivo*.

A.



B.

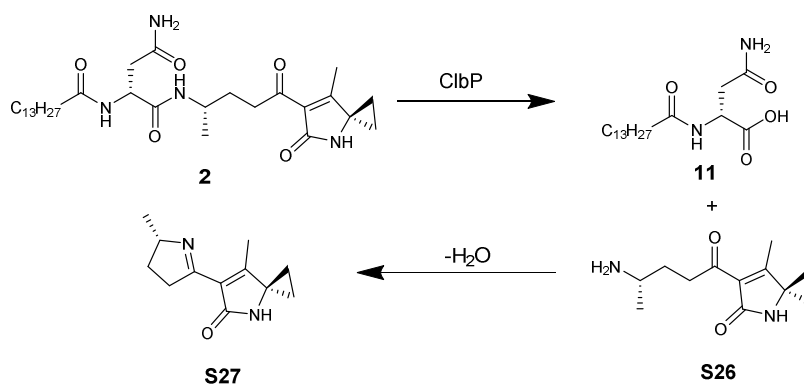


**Figure S3. Cleavage of compound 2 by ClbP.** (A) Cultures of pBAD18 or pCibP were grown to an  $OD_{600}$  of 0.5, and then induced with 0.01% arabinose. Compound 2 was added at a final concentration of 10  $\mu$ M and incubated for four hours. The production of 11, S26, and S27 was monitored and compared to extracts of cultures expressing the full-length pathway. EIC analysis shows that S26 and S27 are also produced by wild-type (pBAC-PKS). The production of these compounds is detailed in part B.



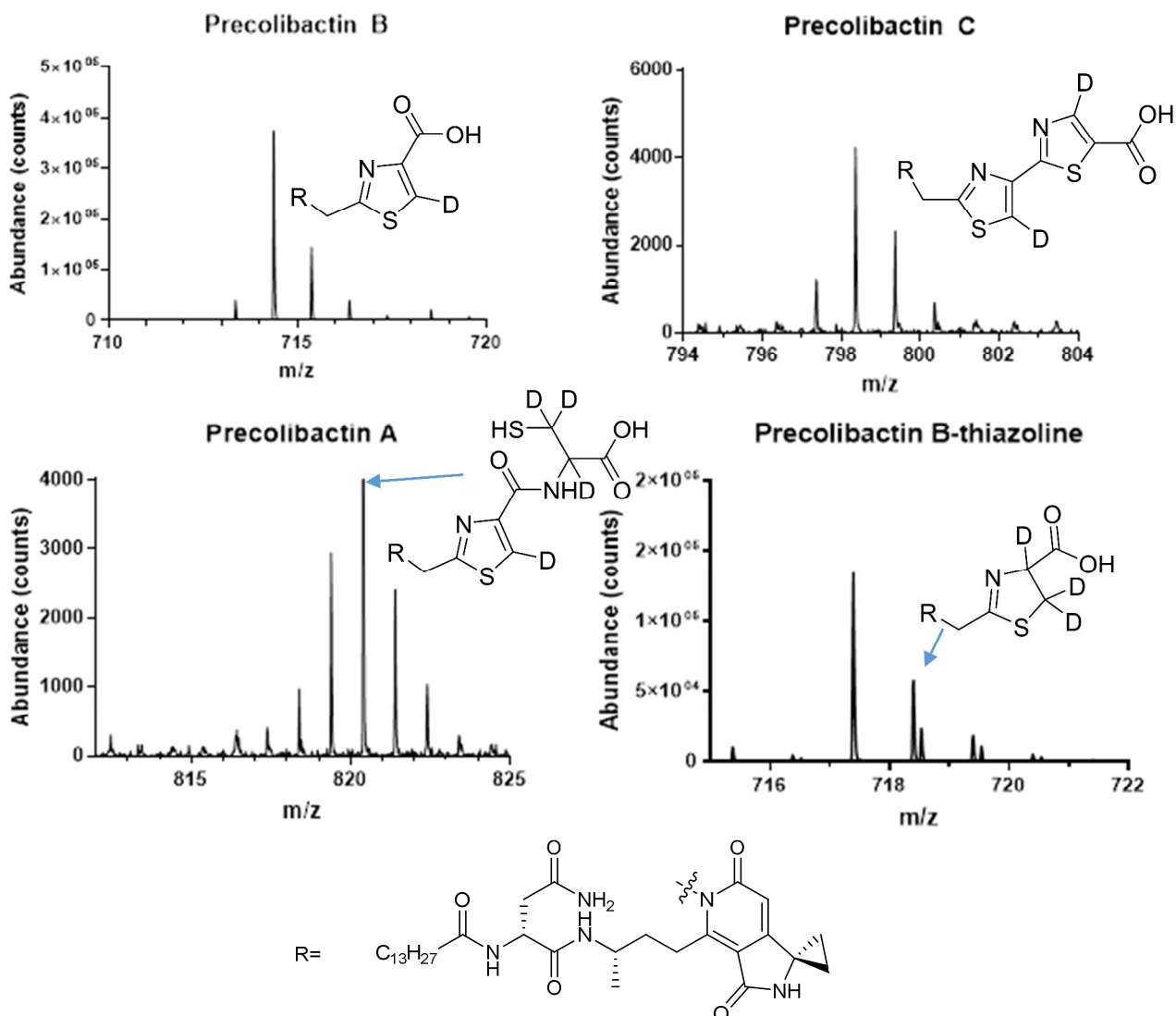


**Figure S4. Incorporation of 2,3,3- $^2\text{H}_3$ -L-cysteine into precolibactins.** Incorporation of the deuterium label occurs as expected for the thiazole-containing precolibactin B and C (top left and right respectively), with one and two deuterium labels being predominantly observed as expected. Ions with masses lacking deuterated cysteine are observed due to competition with naturally produced cysteine. In precolibactin A (bottom left), the predominant species corresponds with a mass of incorporation of 4 deuteriums. However, a species with three deuteriums is observed due to competition with endogenous cysteine as well as some label washout at the  $\alpha$ -carbon. This washout effect is more pronounced in the thiazoline analog of precolibactin B (bottom right) consistent with the increased acidity of its  $\alpha$ -proton (calculated with JChem  $\text{pK}_a$  Calculator 14.8 vs 13.2 for cysteine vs thiazoline). Observation of deuterium signal at the  $\alpha$ -positions support preservation of the L-amino acid configurations.<sup>18</sup>

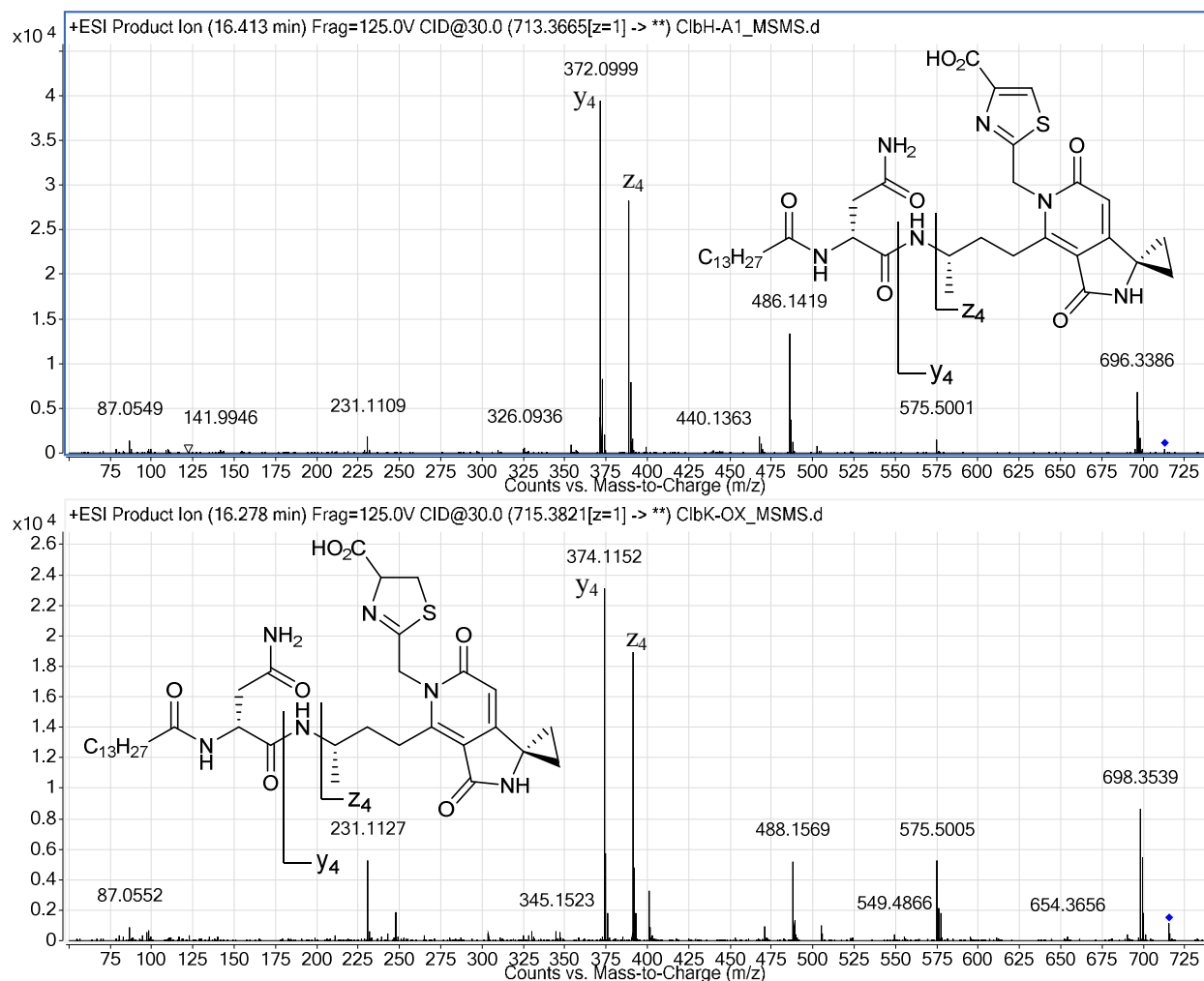


**Figure S5. Comparison of Tandem MS<sup>2</sup> spectra of Precolibactin B and its thiazoline analog.** The fragments containing the pyridone and thiazole in Precolibactin B are shifted by two Daltons, indicating the absence of an oxidation event.

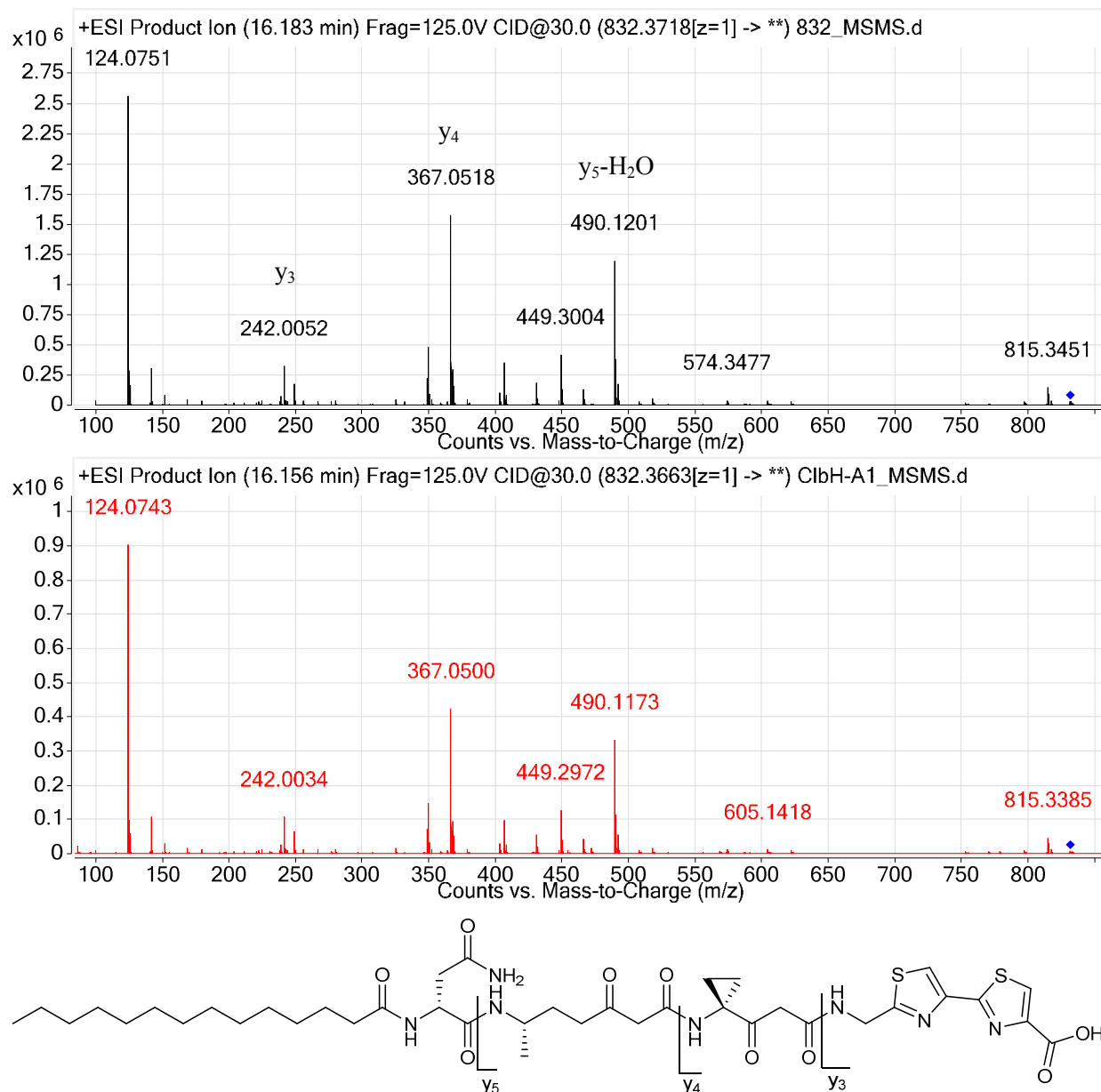
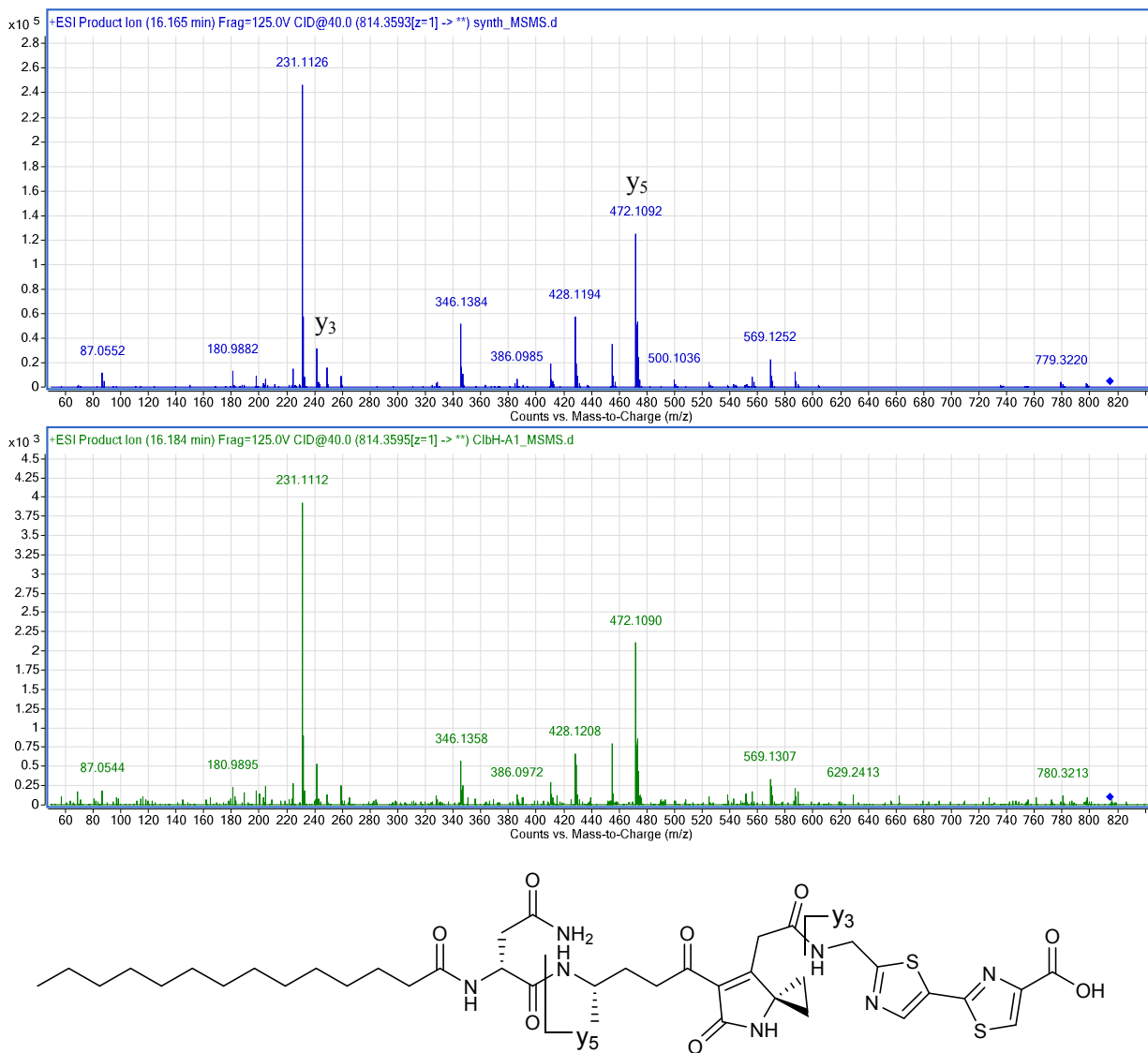
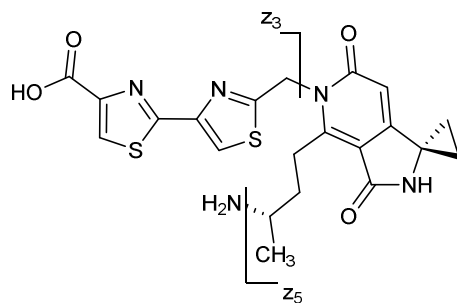
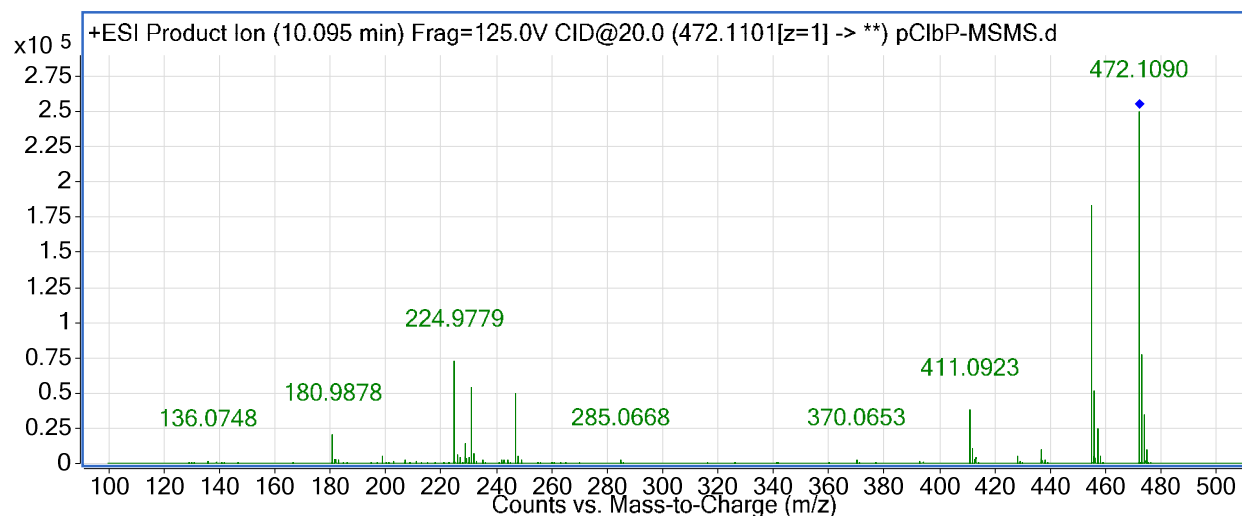
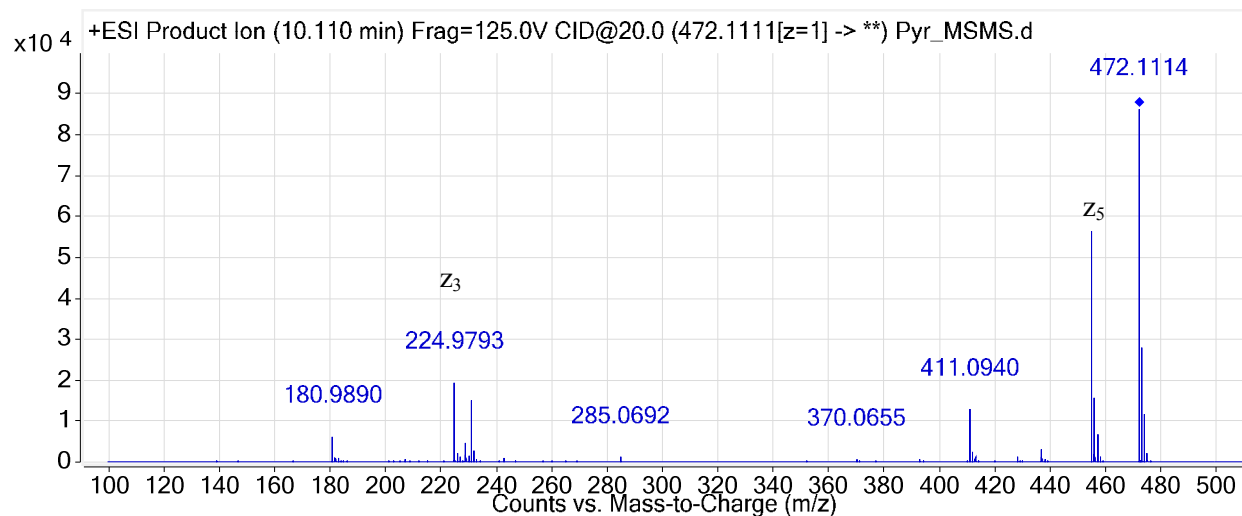


**Figure S6. Comparison of MS/MS spectra of synthetic vs. natural 7.** Tandem MS<sup>2</sup> spectra of synthetic (top, black) vs. natural (bottom, red) 7 are identical. Co-injection also supports structural assignment (Figure 4).



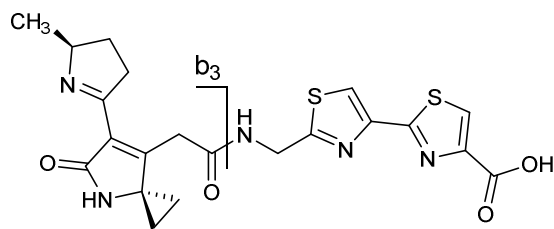
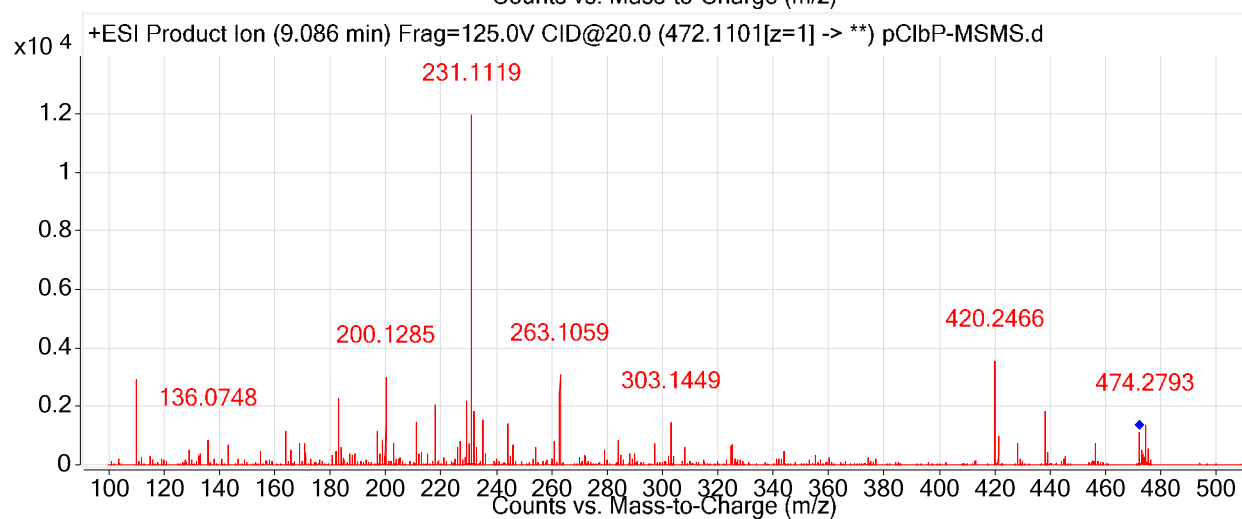
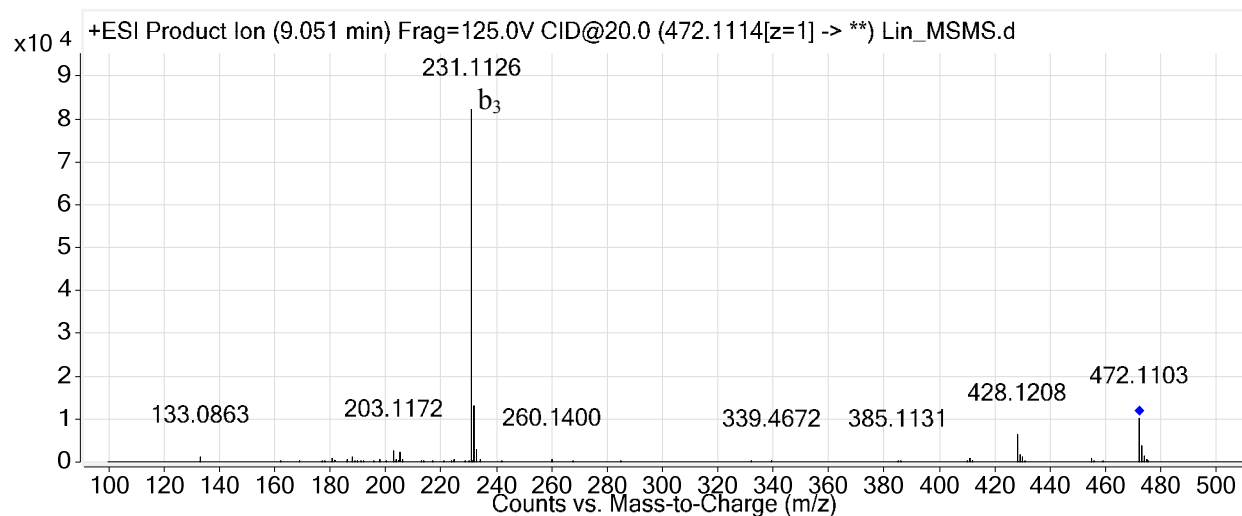
**8**

**Figure S7. Comparison of MS/MS spectra of synthetic vs. natural lactam **8**.** Tandem MS<sup>2</sup> spectra of synthetic (top, blue) vs. natural (bottom, green) **8** are identical. Co-injection experiments also support structural assignment (Figure 4).



9

**Figure S8.** Comparison of MS/MS spectra of **9**. The ClbP-cleaved precolibactin C product **9** was synthesized according to the route previously published<sup>9</sup>. The tandem MS of synthetic **9** matches that of the ClbP-cleaved metabolite.



10

**Figure S9.** Comparison of MS/MS spectra of **10**. Precursor **12** was synthesized according to the route previously published.<sup>9</sup> **10** was generated by cyclizing **12** in saturated sodium bicarbonate as previously described (see Supplementary Methods). The tandem MS of the synthetic material matches that of the material generated by ClbP-cleavage of linear precolibactin C (**7**). Metabolite identification was also supported by co-injection experiments (Figure 5).

## Supplementary References:

- (1) Marahiel, M. A.; Stachelhaus, T.; Mootz, H. D. *Chem. Rev.* **1997**, *97*, 2651.
- (2) Dowling, D. P.; Kung, Y.; Croft, A. K.; Taghizadeh, K.; Kelly, W. L.; Walsh, C. T.; Drennan, C. L. *Proc. Natl. Acad. Sci. U S A* **2016**, *113*, 12432.
- (3) Nougayrede, J. P.; Homburg, S.; Taieb, F.; Boury, M.; Brzuszkiewicz, E.; Gottschalk, G.; Buchrieser, C.; Hacker, J.; Dobrindt, U.; Oswald, E. *Science* **2006**, *313*, 848.
- (4) Gallagher, R. R.; Li, Z.; Lewis, A. O.; Isaacs, F. J. *Nat. Protoc.* **2014**, *9*, 2301.
- (5) Zuker, M. *Nucleic Acids Res.* **2003**, *31*, 3406.
- (6) Datsenko, K. A.; Wanner, B. L. *Proc. Natl. Acad. Sci. U S A* **2000**, *97*, 6640.
- (7) Healy, A. R.; Vizcaino, M. I.; Crawford, J. M.; Herzon, S. B. *J. Am. Chem. Soc.* **2016**, *138*, 5426.
- (8) Pangborn, A. B.; Giardello, M. A.; Grubbs, R. H.; Rosen, R. K.; Timmers, F. J. *Organometallics* **1996**, *15*, 1518.
- (9) Healy, A. R.; Nikolayevskiy, H.; Patel, J. R.; Crawford, J. M.; Herzon, S. B. *J. Am. Chem. Soc.* **2016**, *138*, 15563.
- (10) Guzman, L. M.; Belin, D.; Carson, M. J.; Beckwith, J. *J. Bacteriol.* **1995**, *177*, 4121.
- (11) Vizcaino, M. I.; Engel, P.; Trautman, E.; Crawford, J. M. *J. Am. Chem. Soc.* **2014**, *136*, 9244.
- (12) Vizcaino, M. I.; Crawford, J. M. *Nat. Chem.* **2015**, *7*, 411.
- (13) (a) Bian, X. Y.; Plaza, A.; Zhang, Y. M.; Muller, R. *Chem. Sci.* **2015**, *6*, 3154. (b) Brotherton, C. A.; Wilson, M.; Byrd, G.; Balskus, E. P. *Org. Lett.* **2015**, *17*, 1545.
- (14) Li, Z. R.; Li, Y.; Lai, J. Y.; Tang, J.; Wang, B.; Lu, L.; Zhu, G.; Wu, X.; Xu, Y.; Qian, P. Y. *ChemBioChem* **2015**, *16*, 1715.
- (15) Li, Z. R.; Li, J.; Gu, J. P.; Lai, J. Y. H.; Duggan, B. M.; Zhang, W. P.; Li, Z. L.; Li, Y. X.; Tong, R. B.; Xu, Y.; Lin, D. H.; Moore, B. S.; Qian, P. Y. *Nat. Chem. Biol.* **2016**, *12*, 773.
- (16) (a) Brotherton, C. A.; Balskus, E. P. *J. Am. Chem. Soc.* **2013**, *135*, 3359. (b) Bian, X.; Fu, J.; Plaza, A.; Herrmann, J.; Pistorius, D.; Stewart, A. F.; Zhang, Y.; Muller, R. *ChemBioChem* **2013**, *14*, 1194.
- (17) Engel, P.; Vizcaino, M. I.; Crawford, J. M. *Appl. Environ. Microbiol.* **2014**, *81*, 1502.
- (18) Bode, H. B.; Reimer, D.; Fuchs, S. W.; Kirchner, F.; Dauth, C.; Kegler, C.; Lorenzen, W.; Brachmann, A. O.; Grun, P. *Chem. Eur. J.* **2012**, *18*, 2342.